P517434.PDF

Copy No. 8

DEFENCE R&D DÉFENSE

Theoretical Manual for SEALOADS version 1.1: A Computer Program for Prediction of Nonlinear Ship Motions, Sea Loads, and Pressure Distribution in the Time Domain

W. Qui
H. Peng
C.C. Hsiung

Martec Limited

Martec Limited
1888 Brunswick Street, Suite 400
Halifax, NS
Canada B3J 3J8

Contract #W7707-008063/001/HAL

Contract Scientific Authority: Samon Ando Tele: 426-3100 Ext 203

Defence R&D Canada

Contractor Report
DREA CR 2001-176
August 2001

National Defence Défense nationale

Canada

P517434.PDF [Page: 5 of 91]

104-06254/

Copy No: _____

Theoretical Manual for SEALOADS version 1.1: A Computer Program for Prediction of Nonlinear Ship Motions, Sea Loads, and Pressure Distribution in the Time Domain

W. Qiu
H. Peng
C.C. Hsiung
Martec Limited

Martec Limited
1888 Brunswick Street, Suite 400
Halifax, NS B3J 3J8
Canada

Contract # W7707-008063/001/HAL
Contract Scientific Authority: Samon Ando Tel: 426-3100 Ext 203

Defence Research Establishment Atlantic

Contract Report

CR 2001-176

August 2001

Authors

W. Qiu, H. Peng, and C.C. Hsiung

Approved by

S. Ando

Defence Scientist

Approved for release by

Kirk Foster

DRP Chair

The scientific or technical validity of this Contract Report is entirely the responsibility of the contractor and the contents do not necessarily have the approval or endorsement of Defence R&D Canada

© Her Majesty the Queen as represented by the Minister of National Defence, 2001

© Sa majesté la reine, représentée par le ministre de la Défense nationale, 2001

P517434.PDF [Page: 7 of 91]

Abstract

This report outlines the theoretical background in the FORTRAN program SEALOADS version 1.1 for computing nonlinear ship motions, bending moments and shear forces on the hull, and hydrodynamic pressure distributions over the wetted hull surface. The computation is carried out in the time domain by using the three-dimensional panel method. A pseudo-nonlinear module is introduced to account for the instantaneous wetted surface. In SEALOADS, the external forces acting on the ship hull include the linearized radiation and diffraction forces, nonlinear Froude-Krylov force, viscous roll damping force, bow-flare slamming force and forces from rudder, maneuvering and propeller. The linearized radiation and diffraction forces are obtained from the impulse response functions, which are solved by using the time-domain Green function and applying a non-impulsive input to the ship. The nonlinear Froude-Krylov force is computed at the instantaneous wetted surface of the hull. A two-dimensional wedge model is applied to compute the bow-flare slamming force. The nonlinear equations of ship motion are solved by the fourth-order Runge-Kutta technique or by the extrapolation method. Effects of position-dependent hydrodynamic coefficients are considered. An automatic panel generator based on NURBS surfaces is also included in this version.

Résumé

Ce rapport décrit les fondements théoriques du programme FORTRAN SEALOADS version 1.1, qui sert à calculer les mouvements non linéaires de navires, les moments de flexion et les forces de cisaillement que subit la coque, et la répartition de la pression hydrodynamique sur les surfaces immergées de la coque. Les calculs sont effectués dans le domaine temporel à l'aide de la méthode des panneaux tridimensionnels. Un module pseudo-non linéaire est utilisé pour tenir compte de la surface immergée instantanée. Dans le programme SEALOADS, les forces extérieures qui agissent sur la coque du navire comprennent les forces de radiation et de diffraction linéarisées, la force non linéaire Froude-Krylov, la force de visco-amortissement de roulis, la force de claquement du dévers de l'étrave et les forces provenant du gouvernail, des manœuvres et de l'hélice. Les forces de radiation et de diffraction linéarisées sont obtenues à partir des fonctions de réponse impulsionnelle, qui sont déterminées en utilisant la fonction Green du domaine temporel et en appliquant une entrée non impulsive au navire. La force non linéaire Froude-Krylov est calculée au niveau de la surface immergée instantanée de la coque. Un modèle angulaire bidimensionnel est utilisé pour calculer la force de claquement du dévers de l'étrave. La résolution des équations non linéaires des mouvements du navire se fait par la méthode du quatrième ordre Runge-Kutta ou par extrapolation. Les effets des coefficients hydrodynamiques qui dépendent de la position sont aussi pris en compte. Cette version du programme comprend aussi un générateur de panneaux automatique fondé sur les surfaces NURBS.

P517434.PDF [Page: 8 of 91]

This page intentionally left blank.

P517434.PDF [Page: 9 of 91]

Executive summary

This report outlines the theoretical background in the FORTRAN program SEALOADS version 1.1 for computing nonlinear ship motions, bending moments and shear forces on the hull, and hydrodynamic pressure distributions over the wetted hull surface. The computation is carried out in the time domain by using the three-dimensional panel method. A pseudo-nonlinear module is introduced to account for the instantaneous wetted surface. In SEALOADS, the external forces acting on the ship hull include the linearized radiation and diffraction forces, nonlinear Froude-Krylov force, viscous roll damping force, bow-flare slamming force and forces from rudder, maneuvering and propeller. The linearized radiation and diffraction forces are obtained from the impulse response functions, which are solved by using the time-domain Green function and applying a non-impulsive input to the ship. The nonlinear Froude-Krylov force is computed at the instantaneous wetted surface of the hull. A two-dimensional wedge model is applied to compute the bow-flare slamming force. The nonlinear equations of ship motion are solved by the fourth-order Runge-Kutta technique or by the extrapolation method. Effects of position-dependent hydrodynamic coefficients are considered. An automatic panel generator based on NURBS surfaces is also included in this version. Nonlinear wave loads on ships in severe seas predicted by SEALOADS are useful in determining whether the structure of a Canadian Forces ship could withstand a specified severity of seas with an acceptable risk of failure.

The results show that the computer program SEALOADS provides a practical means for calculating large-amplitude nonlinear loads that are beyond the realm of the conventional linear frequency-domain models.

The extreme loads are a key factor to be considered in the hull structural analysis, but because they occur very rarely, the characteristics of these loads are still poorly understood. SEALOADS serves as a practical analytical tool for examining them.

Future plans include further validation studies, refinement of the algorithms and/or theoretical models to improve the robustness, development of a more advanced method of calculating bow-flare impact force, application of the panel-free method for the computation of radiation and diffraction forces, and development of body-exact algorithm for large-amplitude motions. As well, development of a comprehensive analysis tool for the realistic hydroelastic response of the ship girder based on the framework of SEALOADS is envisaged.

Qiu W, Peng H., and Hsiung C.C. 2001. Theoretical Manual for SEALOADS version 1.1: A Computer Program for Prediction of Nonlinear Ship Motions, Sea Loads, and Pressure Distribution in the Time Domain. DREA CR 2001-176. Defence Research Establishment Atlantic

P517434.PDF [Page: 10 of 91]

Sommaire

Ce rapport décrit les fondements théoriques du programme FORTRAN SEALOADS version 1.1, qui sert à calculer les mouvements non linéaires de navires, les moments de flexion et les forces de cisaillement que subit la coque, et la répartition de la pression hydrodynamique sur les surfaces immergées de la coque. Les calculs sont effectués dans le domaine temporel à l'aide de la méthode des panneaux tridimensionnels. Un module pseudo-non linéaire est utilisé pour tenir compte de la surface immergée instantanée. Dans le programme SEALOADS, les forces extérieures qui agissent sur la coque du navire comprennent les forces de radiation et de diffraction linéarisées, la force non linéaire Froude-Krylov, la force de visco-amortissement de roulis, la force de claquement du dévers de l'étrave et les forces provenant du gouvernail, des manœuvres et de l'hélice. Les forces de radiation et de diffraction linéarisées sont obtenues à partir des fonctions de réponse impulsionnelle, qui sont déterminées en utilisant la fonction Green du domaine temporel et en appliquant une entrée non impulsive au navire. La force non linéaire Froude-Krylov est calculée au niveau de la surface immergée instantanée de la coque. Un modèle angulaire bidimensionnel est utilisé pour calculer la force de claquement du dévers de l'étrave. La résolution des équations non linéaires des mouvements du navire se fait par la méthode du quatrième ordre Runge-Kutta ou par extrapolation. Les effets des coefficients hydrodynamiques qui dépendent de la position sont aussi pris en compte. Cette version du programme comprend aussi un générateur de panneaux automatique fondé sur les surfaces NURBS. Les charges non linéaires des vagues sur les navires en mauvaise mer, prédites par le SEALOADS, sont utiles pour déterminer si la structure d'un navire des Forces pourrait supporter la sévérité prévue de la mer avec un risque acceptable de défaillance.

Les résultats montrent que le programme d'ordinateur SEALOADS fournit des moyens pratiques pour calculer des charges non linéaires qui ne correspondent pas aux modèles du domaine des fréquences linéaires conventionnelles.

Les charges extrêmes sont un facteur dont il faut essentiellement tenir compte dans l'analyse se la structure de la coque, mais comme elles se produisent très rarement, leurs caractéristiques sont très mal connues. Le SEALOADS s'avère un outil d'analyse pratique pour les examiner.

Les futurs plans prévoient d'autres études de validation, un raffinement des algorithmes et/ou des modèles théoriques afin de renforcer la résistance, le développement d'une méthode plus avancée pour calculer la force de choc du dévers de l'étrave, l'application de la méthode sans écran pour calculer les forces de rayonnement et de diffraction et l'élaboration d'algorithmes précis de la coque pour les mouvements à large amplitude. De plus, on envisage de mettre au point un outil servant à analyser la réponse réelle de la poutre navire compte tenu du cadre d'applications de SEALOADS.

Qiu W, Peng H., and Hsiung C.C. 2001. Theoretical Manual for SEALOADS version 1.1: A Computer Program for Prediction of Nonlinear Ship Motions, Sea Loads, and Pressure Distribution in the Time Domain. DREA CR 2001-176. Defence Research Establishment Atlantic

P517434.PDF [Page: 11 of 91]

Contents

Abstract i

List of Figures viii

Nomenclature ix

1 Introduction 1

1.1 Literature Review 1

1.2 Summary of Version 1.1 2

2 Mathematical Formulation 4

2.1 Equations of Ship Motion 4

2.2 The Initial Boundary Value Problem 6

2.3 Linearization 7

2.3.1 The Neumann-Kelvin Linearization 8

2.3.2 The Double-Body Flow 9

2.4 The Boundary Integral Equation 9

2.4.1 Integral Equation in terms of Source Distribution 11

2.5 The Radiation Problem 11

2.5.1 Solution by the Impulse Response Function 13

2.6 The Diffraction Problem 16

2.6.1 Solution Using the Impulse Response Function 17

P517434.PDF [Page: 12 of 91]

3 Pressure Distribution over the Wetted Hull Below DWL 19

3.1 Pressure due to Radiated Waves 19

3.2 Pressure due to Diffracted Waves 20

3.3 Pressure due to Incident Waves 20

4 External Forces and Sea Loads 21

4.1 Froude-Krylov Forces 21

4.2 Bow Flare Impact 22

4.3 Viscous Roll Damping Forces 24

4.3.1 Roll Damping Coefficients Derived from Roll Decay Test 24

4.3.2 Estimates of Roll Damping from Empirical Formulae 26

4.4 Other Viscous Forces and Moments 27

4.4.1 Resistance 27

4.4.2 Cross-Flow Drag 27

4.5 Propeller Thrust 27

4.6 Maneuvering Forces 28

4.7 Rudder Forces and Autopilot 28

4.8 Sea Loads 29

4.8.1 Sea Loads Due to Radiated and Diffracted Waves 30

4.8.2 Sea Loads Due to Incident Waves 30

4.8.3 The Inertial Components of Sea Loads 31

5 Variable Hydrodynamic Coefficients 32

5.1 Review of Literature on the Variability of Hydrodynamic Coefficients 32

5.2 An Automatic Panel Generator 33

5.2.1 NURBS Representation of Hull Form 34

5.2.2 Hull Trimming 35

5.2.3 Panel Generation 37

P517434.PDF [Page: 13 of 91]

6 Concluding Remarks 40

References 42

Appendices 46

A Analytical Solution of the Time-Dependant Green Function 46

B Numerical Solution of the Source Strength from the Integral Equation 52

C Computation of m-terms 54

D Numerical Solution of the Impulse Response Function 56

E Pressure over a Panel due to Incident Waves 58

F Structure of SEALOADS Version 1.1 Code 60

G Examples of Panelized Hull 65

P517434.PDF [Page: 14 of 91]

List of Figures

2.1 Coordinate systems 4
2.2 Definition of wave heading 18

4.1 An impact wedge model (Payne, 1981) 23
4.2 Slamming forces and sign conventions 24

5.1 Example of mean wetted hull surface and the designed waterplane 35
5.2 Control net 36
5.3 Mapping between parametric and physical space 37
5.4 Flat Panel Definition 38

A.1 The Green function and its derivatives in its natural variables (μ,τ) 51

E.1 A quadrilateral panel and the local reference frame 58

F.1 Code structure of SEALOADS Version 1.1 61
F.2 Code structure of Radiation Module 62
F.3 Code structure of Diffraction Module 63
F.4 Code structure of Ship Motion, Pressure and Sea Loads Module 64

G.1 A CPF Hull heeled by port side 2.5°, trimmed 0° and heaved 2.0m 66
G.2 A CPF Hull heeled by port side 1.5°, trimmed by bow 2.5° and heaved 0.0m 67
G.3 A CPF Hull heeled by port side 1.5°, trimmed by stern 2.5° and heaved 0.0m (without transom) 68

P517434.PDF [Page: 15 of 91]

Nomenclature

α	arbitrary constant to control the non-impulsive input motion
α_1^r	yaw gain
α_2^r	yaw rate gain
β	angle of wave propagation relative to the x-axis (180^0 denotes head seas)
β_w	angle of a wedge
Γ	intersection of the mean wetted surface and the still water plane
$\bar{\gamma}_{jk}$	coefficient of hydrodynamic restoring force in the time domain
$\bar{\gamma}_{jk}^f$	coefficient of the hydrodynamic restoring force of the part of the hull from x_e to FP
Δ	weight displacement
$\delta(t-\tau)$	Dirac δ function
δ^r	rudder angle
δ_0^r	threshold value of yaw beyond which the rudder is activated
δ_e^r	effective rudder angle
ϵ_0, ϵ_1	roll damping coefficient
ε_{ijk}	alternating tensor
η	free surface elevation
$\eta_0(t)$	free surface elevation of the incident wave at the origin of the steady-moving coordinate system

P517434.PDF [Page 16 of 91]

$\bar{\eta}_0(t)$	non-impulsive incident wave at the origin of the steady-moving coordinate system
λ_{44}^{ν}	viscous roll damping coefficient corresponding to a frequency of encounter
λ_{BK}	bilge keel roll damping coefficient
λ_E	roll damping coefficient of eddy-making resistance of the hull
λ_F	roll damping coefficient of appendages other than the bilge keel
λ_H	hull frictional roll damping coefficient
$\bar{\lambda}_{jk}$	hydrodynamic damping coefficient in the time domain
$\bar{\lambda}_{jk}^{f}$	damping coefficient of the part of the hull from x_c to FP
$\bar{\lambda}$	aspect ratio of the rudder
$\bar{\mu}_{jk}$	added mass of the ship in the time domain
$\bar{\mu}_{jk}^{f}$	added mass of the part of the hull from x_c to FP
ρ	fluid density
$\sigma(Q;\tau)$	source strength
$\Phi(x,y,z;t)$	total velocity potential of a point (x,y,z) at time t
Φ^{db}	double-body potential function
$\bar{\Phi}$ and $\bar{\phi}$	velocity potential due to the steady translation
ϕ^{db}	the perturbation potential of the uniform stream
ϕ_D or ϕ_7	diffracted wave potential
ϕ_I	incident wave potential
ϕ_k	radiated wave potential in mode k
ψ_k, $\bar{\chi}_k$, φ_k	potential components due to the input motion
Ω	fluid domain
ω	wave frequency
ω_e	frequency of encounter

P517434.PDF [Page: 17 of 91]

A_r	rudder area of a single side
$C_d(x_s)$	sectional cross-flow drag coefficient
d	ship draft
D_p	propeller diameter
d_i	translational displacements in the steady-moving coordinate system
dl_i	length of a segment where the impact occurs
$F(P,Q;t-\tau)$	wave part of the Green function
F_1^{pt}	propeller thrust
F_4^{pt}	propeller torque
$F_{d_k}^s(t)$	sea loads due to diffracted waves
$F_{fk_k}^s(t)$ and $F_{rs_k}^s(t)$	sea loads caused by the incident waves with respect to the Froude-Krylov forces and the restoring forces
$F_{im_k}^s(t)$	sea loads due to bow-flare impact
$F_{in_k}^s(t)$	inertial component of sea loads
$F_k^s(t)$	total sea loads in kth direction
$F_{r_{jk}}^s(t)$	sea loads due to radiated waves
$F^w(t)$	vertical impact force
$F_i^v(t)$	viscous forces
$F_i^{dif}(t)$	diffraction forces
$F_i^{fk}(t)$	Froude-Krylov forces
$F_i^{im}(t)$	bow flare impact forces
$F_i^{mc}(t)$	miscellaneous forces
$F_i^m(t)$	maneuvering forces
$F_i^{pt}(t)$	propeller thrust
$F_i^{rad}(t)$	radiation forces
$F_i^{rs}(t)$	restoring forces

P517434.PDF [Page: 18 of 91]

$F_i^{rud}(t)$	rudder forces
$\bar{F}_i$	external forces acting on the ship
g	acceleration of gravity
$G(P,Q;t-\tau)$	transient Green function
$G_0(P,Q)$	Rankine source
GZ	GZ curve
$H(t-\tau)$	Heaviside unit step function
$\hat{H}(t)$	roll energy of the ship
I_{22}	mass moment of inertia about x-axis
I_{ij}	moment of inertia matrix
J	advancing velocity coefficient
J_0	Bessel function of order zero
k	wave number (except when used as a subscript)
$K_p^D(x,y,z;t)$	pressure response function due to the diffracted waves
$K_{p_k}^R(x,y,z;t)$	pressure response function due to radiated waves
$K_{d_k}^s(t)$	response function of sea loads due to the diffracted waves
K_Q	torque coefficient of propeller
K_T	thrust coefficient of propeller
$K_{j7}^D(t)$	response function for the diffraction force in the jth direction
$K_{jk}^R(t)$	response function of the ship due to the radiated waves
$K_{r_{jk}}^s(t)$	response function of sea loads due to the radiated waves
l_x	horizontal distances between the pressure point C_{rud} and the centre of gravity
l_z	vertical distances between the pressure point C_{rud} and the centre of gravity
l_1	distance between a segment experiencing slamming and a reference section

P517434.PDF [Page: 19 of 91]

m	ship mass
m_f	the mass of the part of the ship between the bow and the cross section x_c
M_t	external bending moments acting on the ship
m_k	kth component of m-terms
n_p	revolution per second of propeller
$\mathbf{n}$	unit vector normal to the body surface
N_ϕ	roll damping coefficient
$o_m x_m y_m z_m$	steady-moving coordinate system
$o_s x_s y_s z_s$	ship-fixed coordinate system
$OXYZ$	space-fixed coordinate system
$p(x, y, z; t)$	pressure
$p_d^I(x, y, z; t)$	dynamic pressure due to incident waves
$p_s^I(x, y, z; t)$	static pressure due to incident waves
$p_D(x, y, z; t)$	pressure due to diffracted waves
$p_I(x, y, z; t)$	pressure due to incident waves
$p_R(x, y, z; t)$	pressure due to radiated waves
r and r_1	distance between the source and field points
$\mathbf{r}_q$	the position vector
$R(e_1)$	roll restoring moment
$S_b^f(t)$	transient wetted surface forward of x_c
$S_b(t)$	transient wetted surface of the body
$\bar{S}_b$	mean wetted surface of the ship
t	time
$T(x_s)$	local draft of the ship
t_0	initial time

P517434.PDF [Page: 20 of 91]

T_{ij}	transformation matrix between the ship-fixed coordinate system and the steady-moving coordinate system
t_p	thrust deduction fraction
U_0	ship forward speed
U_{cx}	longitudinal components of current
U_{cy}	lateral components of current
$\hat{U}$	instantaneous forward speed (the ship's mean forward speed plus the surge velocity)
V_r	relative flow velocity to the rudder
$\mathbf{V}_s(x, y, z; t)$	velocity of the point (x, y, z) on the body surface
$v_2(x_s, t)$	transverse relative velocity between the hull and the water particle of the local cross-flow
$\mathbf{W}$	vector of the steady flow velocity
x_g^f	the x-coordinate of the center of gravity of the ship segment forward of x_c in the ship-fixed frame
x_c	the x-coordinate in the ship-fixed frame of the section considered for sea loads computation
x_g, y_g, z_g	coordinates of the centre of gravity in the ship-fixed coordinate system
x_{m_i}	ship motions in the steady-moving coordinate system
x_i	ship motions in the ship-fixed coordinate system
(X, Y, Z)	coordinates of a point in the space-fixed frame
(x_m, y_m, z_m)	coordinates of a point in the steady-moving frame
(x_s, y_s, z_s)	coordinates of a point in the ship-fixed frame
$Y's$ and $N's$	maneuvering derivatives
z_w, $\dot{z}_w$, $\ddot{z}_w$	vertical displacement, velocity and acceleration of a wedge

Chapter 1

Introduction

A time-domain computer program, SEALOADS version 1.0, has been developed for the Defence Research Establishment Atlantic (DREA). The initial work was described in earlier reports by Cong *et al.* (1999) and Qiu and Hsiung (1999). The code of SEALOADS version 1.0 was modified and enhanced. A new version, version 1.1, includes the effect of variable hydrodynamic coefficients. This manual presents the theoretical background of SEALOADS version 1.1. The algorithm for an automatic panel generator based on Non-Uniform Rational B-Spline surface (NURBS) is also presented.

1.1 Literature Review

The predictions of ship motions, sea loads and hydrodynamic pressure distribution over a ship hull are essential components of ship design. Strip theory has been used as a practical prediction method, but it gives unsatisfactory predictions at low frequencies and at high forward speeds. As well, the strip-theory approach is not able to compute the hydrodynamic pressure distribution over the hull surface. Some of the deficiencies of strip theory can be removed by three-dimensional theory. Several researchers, such as Chang (1977), Inglis and Price (1982) and Guevel and Bougis (1982), have used three-dimensional panels to obtain solutions of ship motion in the frequency domain. The frequency-domain panel method has been employed for ship seakeeping analysis using zero-speed Green function with a "speed correction", since the frequency-domain Green function containing the velocity term is complicated to handle. An alternative approach is to formulate the ship motion problem directly in the time domain. When the forward speed is involved, the time-domain Green function is in a simpler form and requires less computational effort than does the frequency-domain counterpart.

The concept of direct time-domain solution is based on the early work of Finkelstein (1957),

Stoker (1957) and Wehausen and Laitone (1960). Cummins (1962) and Ogilvie (1964) discussed the use of time-domain analysis to solve unsteady ship motion problems The zero forward speed problem has been discussed in detail by Wehausen (1967, 1971).

In the linear time-domain formulations, the time-dependent Green function is applied to derive a boundary-integral equation at the mean wetted surface of the body under the assumptions of small motion and small amplitude incident waves. The linearized radiation and diffraction forces acting on the body can be expressed in terms of convolution integrals of the arbitrary motion with impulse functions. These methods have been developed by Liapis and Beck (1985), Beck and Liapis (1987), Beck and King (1989), Beck and Magee (1990) and Lin and Yue (1994).

Efforts have been made to directly incorporate the nonlinearity into time-domain formulations. One extension of the linear time-domain model is to impose the body boundary condition on the instantaneous wetted surface of the body. The free surface boundary condition remains linear so that the time-dependent Green function can still be applied. The body-exact problem has been solved with various degrees of success by Lin and Yue (1990), Magee (1994) and Danmeier (1999). Huang (1997) combined the exact body boundary condition with a free-surface condition linearized about the incident wave profile. In the results of these studies, the application of the exact body boundary conditions showed promise of improvement for cases of computations dealing with large-amplitude motions.

1.2 Summary of Version 1.1

The linear time-domain model is applied to compute the radiation and diffraction forces. The Froude-Krylov forces and restoring forces are computed on the instantaneous wetted surface under the incident wave profile. The other nonlinear forces such as viscous damping forces and maneuvering forces are also taken into account. A two-dimensional wedge model (Payne, 1981) was applied to compute the bow-flare slamming force. The nonlinear equations of ship motion in SEALOADS can be solved in the time-domain either by the fourth-order Runge-Kutta technique or the Extrapolation Method (Magee, 1994). The uniqueness of the code is that a direct solution approach (Cong *et al.*, 1999) is applied to solve the impulse response function, and the analytical solution of the zero-speed time-dependent Green function is computed by solving an ordinary differential equation (Clement, 1998).

As one further step to improve the computation of ship motions, sea loads and pressures, the variable added mass, damping and restoring forces are taken into account. In this scheme, a series of instantaneous positions of ship are chosen for varied heave, roll and pitch motions. The added mass, damping and restoring coefficients are computed corresponding to each position. A position-dependent matrix is formed (Ando, 2000). In SEALOADS Version 1.1, the instantaneous added-mass, damping and restoring forces are interpolated from the pre-computed matrix based on ship motions at the previous time step.

Chapter 2 describes the nonlinear equations of ship motion, the initial boundary-value problem, and the linearized radiation and diffraction problems. Pressure distributions over the wetted surface are discussed in Chapter 3. The computation of Froude-Krylov forces, bow-flare impact forces, viscous forces and other nonlinear forces, and the computation of hydrodynamic sea loads are emphasized in Chapter 4. Variable hydrodynamic coefficients are discussed in Chapter 5, and an automatic panel generator is also presented in this Chapter.

P517434.PDF [Page: 24 of 91]

Chapter 2

Mathematical Formulation

2.1 Equations of Ship Motion

Three right-handed coordinate systems (as shown in Figure 2.1) are employed for the ship motion analysis. A *earth-fixed* coordinate system, $OXYZ$, has the OXY plane coinciding with the undisturbed water surface and the Z-axis pointing vertically upward. In the *steady-moving* coordinate system, $o_m x_m y_m z_m$, the $o_m x_m y_m$ plane coincides with the calm water surface and $o_m z_m$ is positive upward. The third coordinate system, $o_s x_s y_s z_s$, is fixed on the ship, and o_s is at the point of intersection of calm water surface, the longitudinal plane of symmetry, and the vertical plane passing through midships. The $o_s x_s y_s$ plane coincides with the undisturbed water surface when the ship is at rest. The positive x_s-axis points toward the bow and the y_s-axis to the port side.

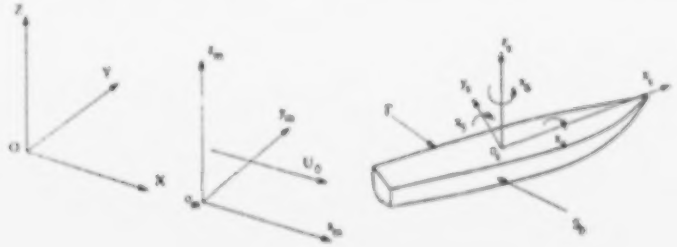

Figure 2.1: Coordinate systems

Denoting a column vector by braces $\{\}$, ship motions in the $o_m x_m y_m z_m$ system are represented by the vector $\mathbf{x}_m = \{x_{m_1}, x_{m_2}, x_{m_3}, x_{m_4}, x_{m_5}, x_{m_6}\}$, in which $\{x_{m_1}, x_{m_2}, x_{m_3}\}$ are the displacements of the center of gravity (CG), and $\{x_{m_4}, x_{m_5}, x_{m_6}\}$ are the Eulerian angles of the ship. The Eulerian angles are the measurements of the ship's rotation about the axes

P517434.PDF [Page: 25 of 91]

which pass through the CG of the ship. The convention for rotational motions are shown in Figure 2.1. The instantaneous translational velocities of ship motion in the directions of $o_s x_s$, $o_s y_s$ and $o_s z_s$ are $\{\dot{x}_1, \dot{x}_2, \dot{x}_3\}$, and the rotational velocities about axes parallel to $o_s x_s$, $o_s y_s$ and $o_s z_s$ and passing through CG are $\{\dot{x}_4, \dot{x}_5, \dot{x}_6\}$. The equations of ship motion are

$$M_{ij}\ddot{x}_j + S_i = F_i, \quad i = 1, 2, ..., 6 \tag{2.1}$$

where $\ddot{\mathbf{x}} = \{\ddot{x}_1, \ddot{x}_2, \ddot{x}_3, \ddot{x}_4, \ddot{x}_5, \ddot{x}_6\}$, $\mathbf{F}$ is the external force vector , and

$$\mathbf{M} = \begin{bmatrix} m & 0 & 0 & 0 & 0 & 0 \\ 0 & m & 0 & 0 & 0 & 0 \\ 0 & 0 & m & 0 & 0 & 0 \\ 0 & 0 & 0 & I_{11} & 0 & -I_{13} \\ 0 & 0 & 0 & 0 & I_{22} & 0 \\ 0 & 0 & 0 & -I_{13} & 0 & I_{33} \end{bmatrix} \tag{2.2}$$

$$\mathbf{S} = \begin{Bmatrix} m(\dot{x}_5\dot{x}_3 - \dot{x}_6\dot{x}_2) \\ m(\dot{x}_6\dot{x}_1 - \dot{x}_4\dot{x}_3) \\ m(\dot{x}_4\dot{x}_2 - \dot{x}_5\dot{x}_1) \\ \dot{x}_5\dot{x}_6(I_{33} - I_{22}) - I_{13}\dot{x}_4\dot{x}_5 \\ \dot{x}_4\dot{x}_6(I_{11} - I_{33}) - I_{13}(\dot{x}_6^2 - \dot{x}_4^2) \\ \dot{x}_4\dot{x}_5(I_{22} - I_{11}) + I_{13}\dot{x}_5\dot{x}_6 \end{Bmatrix} \tag{2.3}$$

where m is the ship mass and I_{ij} is the moment of inertia.

The total external force acting on the ship is

$$F_i = F_i^{rad} + F_i^{dif} + F_i^{fk} + F_i^{rs} + F_i^{v} + F^{w} + F_i^{mc}, \quad \text{for} \quad i = 1, 2, ..., 6 \tag{2.4}$$

where F_i^{rad} and F_i^{dif} are the radiation and diffraction forces, respectively; the F_i^{fk} are the nonlinear Froude-Krylov forces; the F_i^{rs} are the restoring forces; the F_i^{v} are the viscous forces; F_i^{w} the bow-flare slamming force; and the F_i^{mc} are the miscellaneous forces which include the propeller thrust, the maneuvering forces, and the rudder forces. The computation of these forces are described in the following sections and Chapter 4.

The velocities of motions in the $o_m x_m y_m z_m$ system are related to those in the $o_s x_s y_s z_s$ system as follows:

$$\dot{x}_{m_i} = T_{ij}\dot{x}_j, \quad i = 1, 2, ..., 6 \tag{2.5}$$

where $\dot{\mathbf{x}}_m$ represents the ship perturbation velocities in the steady-moving coordinate system. The transformation matrix $\mathbf{T}$ is

P517434.PDF [Page: 26 of 91]

$$\mathbf{T} = \begin{bmatrix} \mathbf{R} & \mathbf{0} \\ \mathbf{0} & \mathbf{B} \end{bmatrix} \tag{2.6}$$

where

$$\mathbf{R} = \begin{bmatrix} c_2c_3 & s_1s_2c_3 - c_1s_3 & c_1s_2c_3 + s_1s_3 \\ c_2s_3 & s_1s_2s_3 + c_1c_3 & c_1s_2s_3 - s_1c_3 \\ -s_2 & s_1c_2 & c_1c_2 \end{bmatrix} \tag{2.7}$$

and

$$\mathbf{B} = \begin{bmatrix} 1 & s_1t_2 & c_1t_2 \\ 0 & c_1 & -s_1 \\ 0 & s_1/c_2 & c_1/c_2 \end{bmatrix} \tag{2.8}$$

where $c_i = \cos(x_i)$, $s_i = \sin(x_i)$ and $t_i = \tan(x_i)$ for i=4, 5 and 6.

Ship motions in the steady-moving coordinate system can be solved from Equations (2.1) and (2.5) either by the Runge-Kutta scheme or by the extrapolation method (Magee, 1994).

2.2 The Initial Boundary Value Problem

It is assumed that the fluid is incompressible, inviscid and free of surface tension and that the flow is irrotational. Consider a three-dimensional body in a semi-infinite fluid with a free surface (see Figure 2.1). The ship moves in an incident wave field with a constant speed U_0 and is allowed to perform small unsteady oscillations about its mean positions in six-degrees of freedom.

Under the above assumptions, the fluid velocity of a point (x, y, z) at time t can be described by the gradient of a scalar velocity potential,

$$\mathbf{V}(x, y, z; t) = \nabla\Phi(x, y, z; t), \tag{2.9}$$

Conservation of mass requires that the velocity potential satisfies the Laplace equation in the fluid domain Ω,

$$\nabla^2\Phi = 0 \tag{2.10}$$

The pressure $p(x, y, z; t)$ in the fluid is given by Bernoulli's equation,

P517434.PDF [Page: 27 of 91]

$$p(x,y,z;t) = -\rho(\Phi_t + \frac{1}{2}V^2 + gz_0) + p_a \tag{2.11}$$

where g is the acceleration of gravity; ρ is the fluid density; p_a is the atmosphere pressure (constant); Φ_t denotes the differentiation of Φ with time t. By setting $p_a = 0$, the free surface boundary condition may be written as

$$\Phi_{tt} + 2\nabla\Phi\cdot\nabla\Phi_t + \frac{1}{2}\nabla\Phi\cdot\nabla(\nabla\Phi\cdot\nabla\Phi) + g\Phi_{z_0} = 0, \quad \text{on } z_0 = \eta \tag{2.12}$$

where $\eta(x_0, y_0; t)$ is the unknown free surface elevation. Two initial conditions are

$$\left.\begin{array}{l}\Phi = 0\\ \Phi_t = 0\end{array}\right\} \quad \text{on } z_0 = 0,\ t \le t_0 \tag{2.13}$$

where t_0 is the starting time for the fluid motions which is zero in the radiation problem and $-\infty$ in the diffraction problem.

On the submerged part of the hull, the no flux body-boundary condition must be satisfied,

$$(\nabla\Phi - \mathbf{V}_s)\cdot\mathbf{n} = 0 \quad \text{on } S_b(t) \tag{2.14}$$

where $\mathbf{V}_s(x,y,z;t)$ is the velocity of the point (x,y,z) on the body surface; $\mathbf{n}$ is the unit inner normal vector to the body surface; and $S_b(t)$ is the instantaneous wetted surface of the body. Fluid motions caused by the body will go to zero at spatial infinity for all finite time,

$$\nabla\Phi \to 0, \quad R_1 = \sqrt{x^2+y^2} \to \infty, \quad \text{for } t < \infty \tag{2.15}$$

2.3 Linearization

It is assumed that the fluid disturbances due to the steady forward motion and the unsteady oscillations are small and can be separated. Then both the free surface and the body boundary conditions, as well as the Bernoulli equation can be linearized. The total velocity potential, in the ship-fixed coordinate system, can be decomposed as follows:

$$\Phi(x,y,z;t) = \bar{\Phi}(x,y,z) + \bar{\phi}(x,y,z) + \sum_{k=1}^{6}\phi_k(x,y,z;t) + \phi_I(x,y,z;t) + \phi_D(x,y,z;t) \tag{2.16}$$

P517434.PDF [Page: 28 of 91]

where the combination of $\bar{\Phi}$ and $\bar{\phi}$ is the velocity potential due to the steady translation for $\bar{\Phi}$ denotes the uniform flow and $\bar{\phi}$ denotes the steady perturbation potential, respectively. This is referred as the *steady* problem. The *radiation* problem is caused by a ship moving in six degrees of freedom. The radiation potential in the kth mode, for $k = 1, 2, \cdots, 6$, is denoted by ϕ_k. The potential of the incident waves is denoted by ϕ_I. For the *diffraction* problem, we denote ϕ_D or ϕ_7 as the potential due to the diffracted waves. Note that in the steady-moving system, the fluid velocity in the far field consists of the uniform flow and the undisturbed incident wave. Far from the ship, the basis flow must tend to the uniform flow, and this potential is assumed to represent the steady flow around the ship. There are two common choices of basis flow: the uniform flow and the double-body flow.

2.3.1 The Neumann-Kelvin Linearization

The choice of a uniform flow alone, i.e., $\bar{\Phi} = -U_0 x$, leads to the Neumann-Kelvin approximation, where the pressure, the free-surface condition and the body boundary condition are given by:

$$p = -\rho(\phi_t - U_0\phi_x) \tag{2.17}$$

$$(\frac{\partial}{\partial t} - U_0\frac{\partial}{\partial x})^2\phi + g\frac{\partial\phi}{\partial z} = 0, \quad \text{on } z = 0 \tag{2.18}$$

$$\mathbf{n}\cdot\nabla(\phi_I + \phi_D) = 0 \quad \text{on } \bar{S}_b \tag{2.19}$$

$$\mathbf{n}\cdot\nabla\phi_k = n_k\dot{x}_k + m_k x_k \quad \text{on } \bar{S}_b \tag{2.20}$$

In equations (2.17) and (2.18), ϕ represents any of the perturbation potentials. $\bar{S}_b$ is the mean wetted surface, and the generalized unit normal n_k is defined as

$$(n_1, n_2, n_3) = \mathbf{n} \tag{2.21}$$

$$(n_4, n_5, n_6) = \mathbf{r}\times\mathbf{n} \tag{2.22}$$

The steady and unsteady potential are coupled through the m-terms (Newman, 1978) in the body boundary conditions. In the Neumann-Kelvin linearization, the m-terms are simplified to

$$m_k = (0, 0, 0, 0, U_0 n_3, -U_0 n_2) \tag{2.23}$$

P517434.PDF [Page: 29 of 91]

2.3.2 The Double-Body Flow

The Neumann-Kelvin linearization works well for slender bodies. However, for more full-formed bodies, the approximation of the body boundary conditions are not satisfactory. As an alternative choice to improve the body-boundary condition, the double-body approximation includes a perturbation of the uniform stream. Then, the steady potential is

$$\Phi^{db} = -U_0 x + \phi^{db}, \tag{2.24}$$

which satisfies the following boundary-value problem,

$$\begin{aligned} \nabla^2 \Phi^{db} &= 0 && \\ \frac{\partial \Phi^{db}}{\partial z} &= 0 && \text{on } z = 0 \\ \mathbf{n} \cdot \nabla \Phi^{db} &= 0 && \text{on } \bar{S}_b \\ \nabla \Phi^{db} &\to (-U_0, 0, 0) && \text{as } R_1 \to \infty \end{aligned} \tag{2.25}$$

According to Newman (1978), the double-body m-terms can be written as

$$\begin{aligned} (m_1, m_2, m_3) &= -(\mathbf{n} \cdot \nabla)\nabla \Phi^{db} \\ &= -(n_1 \Phi^{db}_{xx} + n_2 \Phi^{db}_{xy} + n_3 \Phi^{db}_{xz},\ n_1 \Phi^{db}_{yx} + n_2 \Phi^{db}_{yy} + n_3 \Phi^{db}_{yz}, \\ &\quad n_1 \Phi^{db}_{zx} + n_2 \Phi^{db}_{zy} + n_3 \Phi^{db}_{zz}) \end{aligned} \tag{2.26}$$

$$\begin{aligned} (m_4, m_5, m_6) &= \mathbf{r}_g \times (m_1, m_2, m_3) - \mathbf{n} \times \nabla \Phi^{db} \\ &= \mathbf{r}_g \times (m_1, m_2, m_3) + (n_3 \Phi^{db}_{y} - n_2 \Phi^{db}_{z},\ n_1 \Phi^{db}_{z} - n_3 \Phi^{db}_{x}, \\ &\quad n_2 \Phi^{db}_{x} - n_1 \Phi^{db}_{y}) \end{aligned} \tag{2.27}$$

where $\mathbf{r}_g = (x - x_g, y - y_g, z - z_g)$ is the position vector from the center of gravity (x_g, y_g, z_g) of the ship to a point (x, y, z) on the hull surface. The double-body m-terms, denoted as full m-terms, can be computed using the algorithm given in Appendix C or by solving the integral equation (Huang and Hsiung, 1993).

2.4 The Boundary Integral Equation

The radiation and diffraction problems satisfy the same boundary-value problem with different body boundary conditions. By using the time-dependent Green function the boundary

Ps17434.PDF [Page: 30 of 91]

integral equation can be obtained. The time-dependent Green function satisfies the free-surface, far field, radiation and diffraction conditions, and initial conditions. It can be found in Wehausen and Laitone (1960) or Stoker (1957). By denoting a field point by $P(x, y, z)$, and a source point by $Q(x', y', z')$, the time-dependent Green function for the infinite water depth can be written as

$$G(P, Q; t-\tau) = -\frac{1}{4\pi}[G_0(P, Q)\delta(t-\tau) + H(t-\tau)F(P, Q; t-\tau)] \tag{2.28}$$

with

$$G_0(P, Q) = \frac{1}{r} - \frac{1}{r_1} \tag{2.29}$$

$$\delta(t-\tau) = \begin{cases} 0 & t \neq \tau \\ \infty & t = \tau \end{cases} \tag{2.30}$$

$H(t-\tau)$ is the Heaviside unit step function expressed by

$$H(t-\tau) = \begin{cases} 0 & t < \tau \\ 1 & t \geq \tau \end{cases} \tag{2.31}$$

$$F(P, Q; t-\tau) = 2\int_0^\infty \sqrt{gk}\sin[\sqrt{gk}(t-\tau)]e^{k(z+z')}J_0(kR)dk \tag{2.32}$$

where

$$r = \sqrt{(x-x')^2 + (y-y')^2 + (z-z')^2}, \tag{2.33}$$

$$r_1 = \sqrt{(x-x')^2 + (y-y')^2 + (z+z')^2}, \tag{2.34}$$

$$R = \sqrt{(x-x')^2 + (y-y')^2}, \tag{2.35}$$

and J_0 is the Bessel function of the zeroth order. The zero-speed Green function can be computed by solving the ordinary differential equation derived by Clement(1998). The analytical solution is given in Appendix A. Computation of non-zero speed Green function can be found in the previous reports (Cong *et al.*, 1999).

Applying Green's theorem to the fluid domain Ω, leads to

$$\int\int\int_\Omega (\phi\nabla^2 G - G\nabla^2\phi)d\Omega = \int\int_{S_b} (\phi\frac{\partial G}{\partial n} - G\frac{\partial \phi}{\partial n})dS \tag{2.36}$$

P517434.PDF [Page: 31 of 91]

Integrating both sides of Eq.(2.36) with respect to τ from 0 to t and using the properties of $G(P,Q;t-\tau)$ and the fact that the potential ϕ satisfies the Laplace equation everywhere in the fluid domain, results in the potential in the fluid as

$$\begin{aligned}\phi(P,t) &= \int_0^t d\tau \int\int_{S_b} (\phi\frac{\partial G}{\partial n} - G\frac{\partial \phi}{\partial n})dS - \\ &\frac{1}{g}\int_0^t d\tau \oint_\Gamma \left[U_0^2(G\frac{\partial \phi}{\partial x} - \phi\frac{\partial G}{\partial x}) - U_0(G\frac{\partial \phi}{\partial \tau} - \phi\frac{\partial G}{\partial \tau})\right] dl\end{aligned} \tag{2.37}$$

where Γ is the intersection of the mean hull surface and the plane $z = 0$. The positive line integral is in the counter-clockwise direction.

2.4.1 Integral Equation in terms of Source Distribution

The source strength can be applied to avoid spatial derivatives of the potential. Equation (2.37) can be written in the form of a source distribution:

$$\begin{aligned}\phi(P,t) &= \int_0^t d\tau \int\int_{S_b} G(P,Q;t-\tau)\sigma(Q;\tau)dS \\ &+\frac{U_0^2}{g}\int_0^t d\tau \oint_\Gamma n_1 G(P,Q;t-\tau)\sigma(Q;\tau)dl\end{aligned} \tag{2.38}$$

where σ is the source strength which can be solved from

$$\begin{aligned}\frac{\partial \phi(P;t)}{\partial n} = -\frac{1}{2}\sigma(P;t) &+ \int_0^t d\tau \int\int_{S_b} \frac{\partial G(P,Q;t-\tau)}{\partial n}\sigma(Q;\tau)dS \\ &+ \frac{U_0^2}{g}\int_0^t d\tau \oint_\Gamma \left[n_1\frac{\partial G(P,Q;t-\tau)}{\partial n}\sigma(Q;\tau)\right] dl\end{aligned} \tag{2.39}$$

The numerical implementation of (2.39) is presented in Appendix B.

2.5 The Radiation Problem

The radiation problem is subject to the linearized free-surface boundary condition and the body boundary condition. The potential $\phi_k(x,y,z;t)$, for $k = 1,2,...6$, satisfies the following

P517434.PDF [Page: 32 of 91]

equations:

$$
\begin{aligned}
\nabla^2\phi_k &= 0, && \text{in} \quad \Omega \\
(\frac{\partial}{\partial t} - U_0\frac{\partial}{\partial z})^2\phi_k + g\frac{\partial\phi_k}{\partial z} &= 0, && \text{on} \quad \text{the mean free surface } z = 0 \\
\frac{\partial\phi_k}{\partial n} &= n_k\dot{x}_k + m_k x_k, && \text{on} \quad \text{the mean body surface } \bar{S}_b \\
\nabla\phi_k &\to 0 && \text{as} \quad R_1 \to \infty, \quad \text{on } z = 0 \\
\nabla\phi_k &\to 0 && \text{as} \quad z \to -\infty \\
\phi_k = 0,\ \frac{\partial\phi_k}{\partial t} &= 0, && \text{at} \quad t = 0
\end{aligned}
\tag{2.40}
$$

The linearized unsteady pressure is given by

$$
p_k(x, y, z; t) = -\rho\frac{\partial\phi_k}{\partial t} - \rho\mathbf{W}\cdot\nabla\phi_k \tag{2.41}
$$

where $\mathbf{W} = \nabla(-U_0 x + \phi^{db})$ for the double-body flow approximation.

The hydrodynamic forces acting on the ship can be obtained by integrating the pressure over the wetted surface as follows:

$$
F_{jk} = \int\int_{\bar{S}_b} p_k(x, y, z; t) n_j dS = -\rho\int\int_{\bar{S}_b}\frac{\partial\phi_k}{\partial t}n_j dS - \rho\int\int_{\bar{S}_b}(\mathbf{W}\cdot\nabla\phi_k)n_j dS \tag{2.42}
$$

The second term of (2.42) involves derivatives of ϕ_k. These can be eliminated by using the following theorem presented in Ogilvie and Tuck (1969) or Ogilvie (1977):

$$
\int\int_{\bar{S}_b}[m_j\phi_k + n_j(\mathbf{W}.\nabla\phi_k)]dS = -\oint_\Gamma n_j\phi_k(\mathbf{l}\times\mathbf{n})\cdot\mathbf{W}dl \tag{2.43}
$$

where $\mathbf{l}$ is the unit vector tangential to the waterline Γ. Then, the hydrodynamic force can be written as

$$
F_{jk} = -\rho\int\int_{\bar{S}_b}\frac{\partial\phi_k}{\partial t}n_j dS + \rho\int\int_{\bar{S}_b} m_j\phi_k dS + \rho\oint_\Gamma n_j\phi_k(\mathbf{l}\times\mathbf{n})\cdot\mathbf{W}dl \tag{2.44}
$$

P517434.PDF [Page: 33 of 91]

2.5.1 Solution by the Impulse Response Function

Since the initial boundary value problem for radiation has been linearized, the impulse response function can be used to describe the response of the linear system to an arbitrary input. According to the method proposed by Cummins (1962) or Ogilvie (1964), consider that the ship is given an impulsive motion at $t = 0$ in the kth mode with a velocity $\xi_k(t) = \delta(t)$. Then, the body boundary condition becomes

$$\frac{\partial \phi_k}{\partial n} = n_k \delta(t) + m_k H(t) \quad \text{for} \quad k = 1, 2, \cdots, 6 \tag{2.45}$$

The body boundary condition (2.45) suggests that the potential ϕ_k can be decomposed into an impulsive and a memory part such that

$$\phi_k(x, y, z; t) = \psi_k(x, y, z)\delta(t) + \chi_k(x, y, z)H(t) \tag{2.46}$$

here, both ψ_k and χ_k satisfy the body boundary condition (2.45) for all time if we set

$$\begin{aligned} \frac{\partial \psi_k}{\partial n} &= n_k \quad \text{on } \bar{S}_b \\ \frac{\partial \chi_k}{\partial n} &= m_k \quad \text{on } \bar{S}_b \end{aligned} \tag{2.47}$$

The ψ_k problem describes the fluid motion during the impulsive stage and satisfies

$$\begin{aligned} \psi_k &= 0 \quad \text{on} \quad z = 0 \\ \frac{\partial \psi_k}{\partial n} &= n_k \quad \text{on} \quad \bar{S}_b \\ \nabla \psi_k &\to 0 \quad \text{at} \quad \infty \end{aligned} \tag{2.48}$$

The χ_k potential represents the motion of the fluid subsequent to the initial impulse and is composed of two components. The first component accounts for a change of body orientation due to the impulse in velocity. After the impulse in velocity the body will have a unit displacement in the kth mode. Since the body is in the steady flow field, it results in a change of fluid velocity on the body surface. In order to satisfy the body boundary condition, this change must be canceled. Therefore, $\partial \chi_k / \partial n$ must have the value m_k on the body surface for all $t \geq 0$.

P517434.PDF [Page 14 of 91]

The second component is the result of the impulsive velocity inducing a disturbance into the flow field which will propagate as a wave motion away from the body at subsequent times. Therefore, χ_k will satisfy the free surface condition for $t > 0$ and the initial condition,

$$\begin{aligned} \chi_k &= 0 \qquad \text{on} \quad z = 0 \\ \frac{\partial \chi_k}{\partial t} &= -g\frac{\partial \psi_k}{\partial z} \qquad \text{on} \quad z = 0 \end{aligned} \tag{2.49}$$

Considering the two components above, χ_k can be written as

$$\chi_k = \varphi_k H(t) + \bar{\chi}_k \tag{2.50}$$

where φ_k represents the potential caused by the unit displacement during the impulsive stage of the motion. It satisfies the following boundary conditions:

$$\begin{aligned} \frac{\partial \varphi_k}{\partial n} &= m_k \qquad \text{on} \quad \bar{S}_b \\ \varphi_k &= 0 \qquad \text{on} \quad z = 0 \\ \nabla \varphi_k &\to 0 \qquad \text{at} \quad \infty \end{aligned} \tag{2.51}$$

The potential of the second component $\bar{\chi}_k$ satisfies the following conditions:

$$\begin{aligned} \bar{\chi}_k &= 0 && \text{at} \quad t = 0 \\ \frac{\partial \bar{\chi}_k}{\partial t} &= -g\frac{\partial \psi_k}{\partial z} && \text{on} \quad z = 0 \ \text{ at } t = 0 \\ \frac{\partial^2 \bar{\chi}_k}{\partial t^2} &= -g\frac{\partial \varphi_k}{\partial z} && \text{on} \quad z = 0 \ \text{ at } t = 0 \\ \frac{\partial \bar{\chi}_k}{\partial n} &= 0 && \text{on} \quad \bar{S}_b \ \text{ for } t \geq 0 \\ \left[(\frac{\partial}{\partial t} - U_0\frac{\partial}{\partial x})^2 + g\frac{\partial}{\partial z}\right](\bar{\chi}_k + \varphi_k) &= 0 && \text{on} \quad z = 0 \ \text{ for } t \geq 0 \end{aligned} \tag{2.52}$$

Using Eq.(2.50), the potential for an arbitrary forced motion in terms of a velocity , $\dot{\xi}_k(t)$, for the kth mode of motion can be found by integrating Eq.(2.46)

$$\begin{aligned}\phi_k(x,y,z;t) &= \int_0^t \phi_k(x,y,z;\tau)\dot{\xi}_k(t-\tau)d\tau \\ &= \psi_k(x,y,z)\dot{\xi}_k(t) + \varphi_k(x,y,z)\xi_k(t) + \int_0^t \bar{\chi}_k(x,y,z;\tau)\dot{\xi}_k(t-\tau)d\tau\end{aligned} \tag{2.53}$$

Here, $\phi_k(x,y,z;t)$ satisfies the body boundary condition, the free surface condition, and the conditions at infinity for all times (Cummins, 1962). Note that ψ_k, φ_k and $\bar{\chi}_k$ can be solved from equations (2.49), (2.51) and (2.52), respectively.

Substituting Eq.(2.53) into Eq.(2.44), the radiation force can be expressed as:

$$F_{jk} = -\bar{\mu}_{jk}\ddot{\xi}_k(t) - \bar{\lambda}_{jk}\dot{\xi}_k(t) - \bar{\gamma}_{jk}\xi_k(t) - \int_0^t K_{jk}^R(t-\tau)\dot{\xi}_k(\tau)d\tau \tag{2.54}$$

where

$$\begin{aligned}\bar{\mu}_{jk} &= \rho\int\int_{\bar{S}_b}\psi_k n_j dS \\ \bar{\lambda}_{jk} &= \rho\left[\int\int_{\bar{S}_b}\varphi_k n_j dS - \int\int_{\bar{S}_b}\psi_k m_j dS - \oint_\Gamma \psi_k n_j(\mathbf{l}\times\mathbf{n})\cdot\mathbf{W}dl\right] \\ \bar{\gamma}_{jk} &= -\rho\left[\int\int_{\bar{S}_b}\varphi_k m_j dS + \oint_\Gamma \varphi_k n_j(\mathbf{l}\times\mathbf{n})\cdot\mathbf{W}dl\right] \\ K_{jk}^R(t) &= \rho\left[\int\int_{\bar{S}_b}\frac{\partial\bar{\chi}_k}{\partial t}n_j dS - \int\int_{\bar{S}_b}\bar{\chi}_k m_j dS - \oint_\Gamma \bar{\chi}_k n_j(\mathbf{l}\times\mathbf{n})\cdot\mathbf{W}dl\right]\end{aligned}$$

Here, $\bar{\mu}_{jk}$ is the added-mass of the ship in the time domain which depends on the ship geometry; $\bar{\lambda}_{jk}$ is the hydrodynamic damping coefficient depending on the ship geometry and the forward speed; $\bar{\gamma}_{jk}$ is the coefficient of the hydrodynamic restoring force in the time domain, which also depends on the ship geometry and forward speed; $K_{jk}^R(t)$ is a function of ship geometry, speed and time and shows the memory effects of the impulse motion. Note that hydrodynamic coefficients, $\bar{\mu}_{jk}$, $\bar{\lambda}_{jk}$ and $\bar{\gamma}_{jk}$ are computed on the mean wetted surface $\bar{S}_b$.

The impulse response function, K_{jk}^R, can be obtained by using a non-impulsive input velocity:

$$\dot{\xi}_k(t) = \sqrt{\frac{\alpha}{\pi}}e^{-\alpha t^2} \tag{2.55}$$

The use of a non-impulsive input can eliminate the high frequency content of input, thus avoiding numerical problems. Here, α is an arbitrary constant which controls the frequency content of the input. It is easily shown that as $\alpha \to \infty$ the input is identical to $\dot{\xi}_k = \delta(t)$. The input velocity has the following properties:

$$\xi_k(t) = \frac{1}{2}[1 + \mathrm{erf}(\sqrt{\alpha}t)] \tag{2.56}$$

$$\ddot{\xi}_k(t) = -2\alpha t\dot{\xi}_k(t) \tag{2.57}$$

Under this non-impulsive input, the body boundary condition becomes,

$$\frac{\partial\phi_k}{\partial n} = n_k\dot{\xi}_k(t) + m_k\xi_k(t) \tag{2.58}$$

Then, the corresponding $\bar{\mu}_{jk}$, $\bar{\lambda}_{jk}$ and $\bar{\gamma}_{jk}$ can be obtained. Note that the radiation force in Eq.(2.44) can also be written as

$$F_{jk}(t) = -\dot{g}_{jk}(t) - h_{jk}(t) \tag{2.59}$$

with

$$g_{jk} = \rho\int\int_{S_b}\phi_k(t)n_j dS \tag{2.60}$$

$$h_{jk} = -\rho\int\int_{S_b}\phi_k(t)m_j dS - \rho\oint_\Gamma\phi_k(t)n_j(\mathbf{l}\times\mathbf{n})\cdot\mathbf{W}dl \tag{2.61}$$

Comparing Eq.(2.59) and Eq.(2.54) leads to

$$\int_0^t K_{jk}^R(t-\tau)\dot{\xi}_k(\tau)d\tau = \dot{g}_{jk}(t) + h_{jk}(t) - \bar{\mu}_{jk}\ddot{\xi}_k(t) - \bar{\lambda}_{jk}\dot{\xi}_k(t) - \bar{\gamma}_{jk}\xi_k(t) \tag{2.62}$$

where the impulse response function, K_{jk}^R, is solved for a short duration based on the non-impulsive input $\dot{\xi}_k(t)$. The radiation force due to an arbitrary input motion $\dot{x}_k(t)$ then can be obtained from Eq.(2.54), where $\dot{x}_k(t)$ is substituted for $\dot{\xi}_k(t)$. The numerical solution of the impulse response function is given in Appendix D.

2.6 The Diffraction Problem

The linearized diffraction problem can be stated as follows:

$$\nabla^2\phi_7 = 0 \qquad \text{in} \quad \Omega \tag{2.63}$$

P517434.PDF [Page: 37 of 91]

$$
\begin{aligned}
(\frac{\partial}{\partial t} - U_0\frac{\partial}{\partial z})^2\phi_7 + g\frac{\partial \phi_7}{\partial z} = 0, \qquad & \text{on} \quad z = 0 \\
\frac{\partial \phi_7}{\partial n} = -\frac{\partial \phi_I}{\partial n} \qquad & \text{on} \quad \bar{S}_b \\
\nabla\phi_7 \to 0 \qquad & \text{as} \quad R_1 \to \infty, \text{ on } z = 0 \\
\nabla\phi_7 \to 0 \qquad & \text{as} \quad z \to -\infty \\
\phi_7 = 0,\ \frac{\partial \phi_7}{\partial t} = 0 \qquad & \text{as} \quad t \to -\infty
\end{aligned}
$$

where $\phi_7(x, y, z; t)$ denotes the diffracted wave potential.

2.6.1 Solution Using the Impulse Response Function

In a similar way to the radiation problem, we can use a non-impulsive incident wave to determine the diffracted wave force. The exciting forces can be computed from

$$F_{j7} = \int_{-\infty}^{\infty} K_{j7}^D(t-\tau)\eta_0(\tau)d\tau \tag{2.64}$$

where $K_{j7}^D(t)$ is the impulse response function for the diffraction force in the jth mode; $\eta_0(t)$ is the free surface elevation of the incident wave at the origin of the steady-moving coordinate system. The diffraction force can also be expressed as

$$F_{j7}(t) = -\dot{g}_{j7}(t) - h_{j7}(t) \tag{2.65}$$

where

$$g_{j7} = \rho \int\int_{\bar{S}_b} \phi_7(t) n_j dS \tag{2.66}$$

$$h_{j7} = -\rho \int\int_{\bar{S}_b} \dot{\phi}_7(t) m_j dS - \rho \oint_\Gamma \phi_7(t) n_j (1 \times \mathbf{n}) \cdot \mathbf{W} dl \tag{2.67}$$

and $\phi_7(t)$ is solved from Eq.(2.63). The impulse response function $K_{j7}^D(t)$ can be written as

$$\int_{-\infty}^{\infty} K_{j7}^D(t-\tau)\eta_0(\tau)d\tau = -\dot{g}_{j7}(t) - h_{j7}(t) \tag{2.68}$$

For the case of a ship with forward speed, a non-impulsive incident wave at the origin of the steady-moving reference frame can be chosen as,

$$\bar{\eta}_0(t) = \frac{1}{\pi}\mathrm{Re}(\int_0^{\infty} e^{-\omega^2/4\alpha} e^{i\omega_e t} d\omega_e) \tag{2.69}$$

e517434.PDF [Page: 38 of 91]

where α is an arbitrary constant; $\omega_e = \omega - U_0\omega^2/g\cos\beta$ is the frequency of encounter; β is the angle of wave propagation relative to the x-axis, where 180^0 denotes head seas (see Figure 2.2); ω is the wave frequency. Corresponding to the non-impulsive wave elevation, the derivatives of the incident wave potential can be obtained as

$$\nabla\bar{\phi}_0(x,y,z;t) = \frac{1}{\pi}\mathrm{Re}\left(\left\{\begin{array}{c}\cos\beta\\ \sin\beta\\ i\end{array}\right\}\int_0^\infty \omega e^{k(z-i\varpi)}e^{-\omega^2/4\alpha}e^{i\omega_e t}d\omega_e\right) \tag{2.70}$$

where $\varpi = x\cos\beta + y\sin\beta$ and $k = \omega^2/g$, the wave number. Details on the original derivation of $\bar{\eta}_0$ and $\nabla\bar{\phi}_0$ were given by King, Beck and Magee (1988).

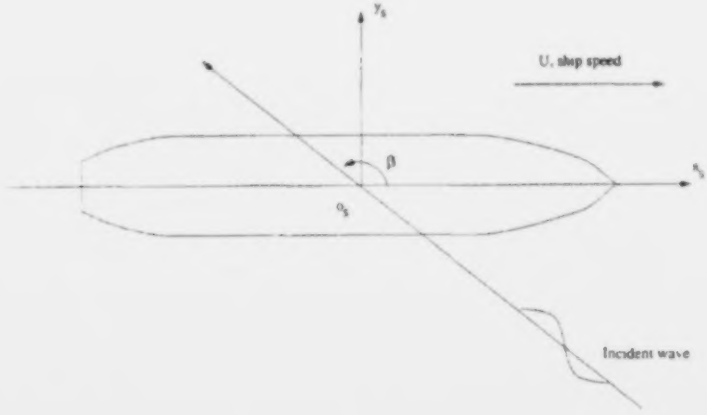

Figure 2.2: Definition of wave heading

With the non-impulsive incident wave $\bar{\eta}_0$, the body boundary condition in Eq.(2.63) becomes

$$\frac{\partial\phi_7}{\partial n} = -\frac{\partial\bar{\phi}_0}{\partial n} \tag{2.71}$$

The respective $\dot{g}_{ij}(t)$ and h_{j7} can be obtained from Eq.(2.66) and Eq.(2.67) by solving Eq.(2.63). Then, the impulse response function $K_{j7}^D(t)$ can be solved from the following equation:

$$\int_{-\infty}^{\infty} K_{j7}^D(t-\tau)\bar{\eta}_0(\tau)d\tau = -\dot{g}_{j7}(t) - h_{j7}(t) \tag{2.72}$$

P517434.PDF [Page: 39 of 91]

Chapter 3

Pressure Distribution over the Wetted Hull Below DWL

The pressure at a point (x, y, z) on the wetted hull below DWL can be expressed as

$$p(x, y, z; t) = p_R(x, y, z; t) + p_D(x, y, z; t) + p_I(x, y, z; t) + \delta p_s(x, y, z; t) \tag{3.1}$$

where $p_I(x, y, z; t)$ and $p_D(x, y, z; t)$ are the pressures due to the incident waves and the diffracted waves, respectively; $\delta p_s(x, y, z; t)$ is the hydrostatic pressure fluctuation due to the oscillatory ship motion. The pressure $p_R(x, y, z; t)$ due to the radiated waves is given by

$$p_R(x, y, z; t) = \sum_{k=1}^{6} p_k^R(x, y, z; t) \tag{3.2}$$

3.1 Pressure due to Radiated Waves

For the linearized radiation problem, the pressure at a point (x, y, z) in the kth mode of motion, $p_k^R(x, y, z; t)$, can be related to an input velocity $\dot{x}_k(t)$ by

$$p_k^R(x, y, z; t) = \int_0^t K_{p_k}^R(x, y, z; t - \tau)\dot{x}_k(\tau)d\tau \tag{3.3}$$

where $K_{p_k}^R(x, y, z; t - \tau)$ is the pressure response function due to the motion. It can be solved

P517434.PDF [Page: 40 of 91]

by using the non-impulsive input given by Eq.(2.55). The pressure corresponding to the non-impulsive input $\bar{\xi}_k$ can be obtained from Eq.(2.41). The numerical solution is similar to that of K_{jk}^R (Eq. 2.62).

3.2 Pressure due to Diffracted Waves

In a similar way to the solution of the radiation pressure, the pressure due to the diffracted waves can also be defined by a convolution product of the pressure response function, $K_p^D(x, y, z; t)$, and the wave elevation at the origin of the steady-moving system, $\eta_0(t)$, as follows:

$$p_D(x, y, z; t) = \int_{-\infty}^{\infty} K_p^D(x, y, z; t - \tau)\eta_0(\tau)d\tau \tag{3.4}$$

The response function $K_p^D(x, y, z; t - \tau)$ is solved by using the non-impulsive input $\bar{\eta}_0(t)$ as given in Eq.(2.69).

3.3 Pressure due to Incident Waves

In an incident field, the wave profile $\eta(X, Y; t)$ at any point on the hull surface can be computed in the earth-fixed coordinate system as follows:

$$p_I(X, Y, Z; t) = p_I^s(X, Y, Z; t) + p_I^d(X, Y, Z; t) \tag{3.5}$$

where the static pressure is

$$p_I^s(X, Y, Z; t) = -\rho g[Z - \eta(X, Y; t)] \tag{3.6}$$

and the dynamic pressure is

$$p_I^d(X, Y, Z; t) = -\rho\frac{\partial\phi_I(X, Y, Z; t)}{\partial t} - \frac{1}{2}\rho|\nabla\phi_I(X, Y, Z; t)|^2 \tag{3.7}$$

and (X, Y, Z) is a point in the earth-fixed coordinate system. The elevations and potentials of regular and irregular waves used in the current work are briefly outlined in the corresponding User's guide (Qiu *et al.*, 2001).

P517434.PDF [Page: 41 of 91]

Chapter 4

External Forces and Sea Loads

This chapter describes the computation of the external forces including the Froude-Krylov forces, bow-flare impact forces, viscous forces and other nonlinear forces. The computation of linear radiation and diffraction forces was introduced in Chapter 2. The computational scheme for sea loads at a specific section is also presented.

4.1 Froude-Krylov Forces

At each time step, the instantaneous position of any point on the surface of the hull can be computed in the steady-moving coordinate system as follows:

$$\begin{pmatrix} x_m \\ y_m \\ z_m \end{pmatrix} = \begin{pmatrix} d_1 + x_g \\ d_2 + y_g \\ d_3 + z_g \end{pmatrix} + [R_{ij}] \begin{pmatrix} x_s - x_g \\ y_s - y_g \\ z_s - z_g \end{pmatrix}, \quad i, j = 1, 2, 3 \tag{4.1}$$

where (x_m, y_m, z_m) are the coordinates of a point in the steady-moving coordinate system; (x_g, y_g, z_g) are coordinates of the center of gravity in the ship-fixed coordinate system; (d_1, d_2, d_3) are translational displacements along x_m-, y_m- and z_m-axis, respectively, in the steady-moving coordinate system; and (x_s, y_s, z_s) are the coordinates of a point in the ship-fixed coordinate system. $[R_{ij}]$ is the transformation matrix between the ship-fixed coordinate system and the steady-moving coordinate system. The corresponding point in the earth-fixed system, (X, Y, Z), can be expressed as

$$\begin{pmatrix} X \\ Y \\ Z \end{pmatrix} = \begin{pmatrix} U_0 t + x_m \\ y_m \\ z_m \end{pmatrix} \tag{4.2}$$

PS17434.PDF [Page: 42 of 91]

At each time step, the instantaneous position of the hull in the space-fixed system can be obtained from Eq.(4.1) and Eq.(4.2). The pressure at any point of the hull up to the superstructure can be computed from Eq.(3.5).

In the current work, quadrilateral panels are used to discretize the ship's hull. Assuming that the pressure is linearly distributed over a panel, the pressure due to the incident waves at a point on a panel can be expressed as

$$\bar{p}_I(X,Y,Z,t) = \sum_{i=1}^{4} N_i(X,Y,Z) p_{I_i}(X,Y,Z) \tag{4.3}$$

Where N_i is the shape function at node i; p_{I_i} is the pressure at node i. The details of computation are given in Appendix E.

The restoring forces are obtained as

$$F_k^{I^s}(t) = -\int\int_{S_b(t)} \bar{p}_I^s n_k dS \tag{4.4}$$

and the nonlinear Froude-Krylov forces are

$$F_k^{fk}(t) = -\int\int_{S_b(t)} \bar{p}_I^d n_k dS \tag{4.5}$$

where $\bar{p}_I^s$ and $\bar{p}_I^d$ are the static and dynamic pressure of a point on a panel, which can be obtained from Equations (3.6), (3.7) and (4.3), respectively.

4.2 Bow Flare Impact

The model for the two-dimensional vertical impact of a wedge in a fluid (Payne, 1981) is applied to the bow-flare impact analysis. Assuming the conservation of momentum in a dynamic system, the vertical impact force acting on a wedge of a unit length is expressed as

$$F^w(t) = \frac{\pi \rho z_w f(\beta_w)}{\tan^2 \beta_w} (\dot{z}_w^2 + \frac{1}{2} z_w \ddot{z}_w) \tag{4.6}$$

where $F^w(t)$ is the vertical impact force; z_w, $\dot{z}_w$ and $\ddot{z}_w$ are the vertical displacement, velocity and acceleration of the wedge, respectively, relative to the water surface; and β_w is

P517434.PDF [Page: 43 of 91]

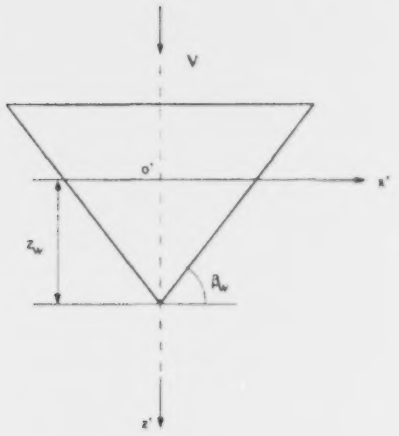

Figure 4.1: An impact wedge model (Payne, 1981)

the deadrise angle of the wedge as illustrated in Figure 4.1. In the figure, a moving local coordinate system $o'x'z'$ is introduced. The $o'x'$ axis is on the still water surface. The $o'z'$ axis coincides with the centerline of the wedge and is positive upward. The instantaneous position of the wedge angle is used at each time step (Qiu *et al.*, 1997).

The vertical shear force and bending moment at a given section caused by the bow-flare impact is computed as

$$F_3^{im}(t) = \sum_{i=1}^{n} F_i^w(t) dl_i \tag{4.7}$$

$$F_5^{im}(t) = \sum_{i=1}^{n} F_i^w l_i dl_i \tag{4.8}$$

where $F_3^{im}(t)$ and $F_5^{im}(t)$ are the total vertical shear force and bending moment, respectively, due to the bow-flare impact; n is the total number of cross section where impact will occur; $F_i^w(t)$ is the vertical slamming force acting on a segment i per unit length; dl_i is the length of the segment and l_i is the distance between a segment experiencing slamming and a reference section. These variables and the force sign conventions are shown in Figure 4.2. Note that the slamming forces are first computed in the earth-fixed coordinate system, and then are transferred to the ship-fixed coordinate system.

P517434.PDF [Page: 44 of 91]

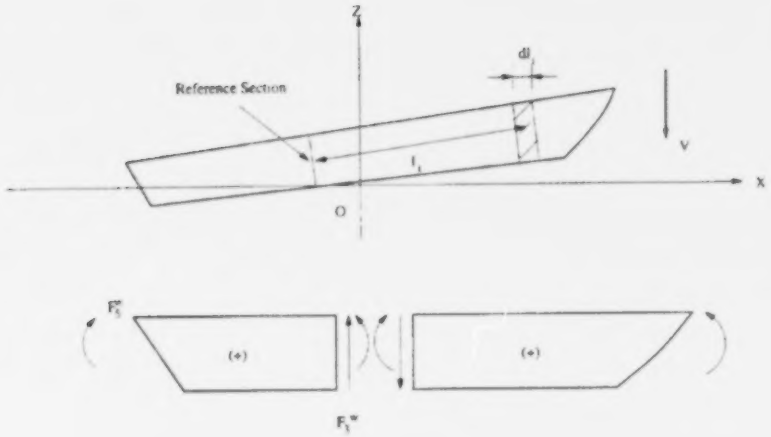

Figure 4.2: Slamming forces and sign conventions

4.3 Viscous Roll Damping Forces

The viscous roll damping forces can be obtained either from empirical formulae or from roll test decay tests.

4.3.1 Roll Damping Coefficients Derived from Roll Decay Test

If roll decay test results are available, the energy method (Haddara and Bennett, 1989) can be used to compute the viscous roll damping coefficient. The energy method states that the rate of change of total energy in the rolling motion is equal to the ratio of energy dissipated by the roll damping. The equation of roll motion, consistent with Eq.(2.1), can be written as

$$(I_{11} + \Delta I_{11})\ddot{x}_4 + 2N_\phi \dot{x}_4 + R(x_4) = 0 \tag{4.9}$$

where x_4 is the roll angle; I_{11} is the mass moment of inertia about x-axis; ΔI_{11} is the added mass moment of inertia; N_ϕ is the roll damping coefficient. The overdots indicate differentiation with respect to time, and $R(x_4)$ is the restoring moment.

Multiplying both sides of Eq.(4.9) by $\dot{x}_4$ and integrating the equation from t_i to t_{i+1}, we obtain

P517434.PDF [Page: 45 of 91]

$$\hat{H}(t_i) - \hat{H}(t_{i+1}) = 2\int_{t_i}^{t_{i+1}} N_\phi \dot{x}_4^2 dt \tag{4.10}$$

where $\hat{H}(t)$, the roll energy of the ship, can be written as

$$\hat{H}(t) = \frac{1}{2}(I_{11} + \Delta I_{11})\dot{x}_4^2 + \Delta \int_0^{x_4} GZ(\zeta)d\zeta \tag{4.11}$$

where the last term stands for the potential energy, which is computed from the GZ curve; Δ is the weight displacement. The general form of the damping coefficient is expressed as

$$N_\phi = \epsilon_0 + \epsilon_1|x_4| + \epsilon_2 x_4^2 + \epsilon_3|\dot{x}_4| + \dot{\epsilon}_2 x_4^2 \tag{4.12}$$

Then Eq.(4.10) is rewritten as

$$\hat{H}(t_i) - \hat{H}(t_{i+1}) = \sum_{j=0}^{4} \alpha_j U_{ij} \tag{4.13}$$

where

$$\begin{aligned}
\alpha_j &= 2\epsilon_j \qquad (4.14)\\
U_{i0} &= \int_{t_i}^{t_{i+1}} \dot{x}_4^2(t)dt\\
U_{i1} &= \int_{t_i}^{t_{i+1}} \dot{x}_4^2(t)|x_4(t)|dt\\
U_{i2} &= \int_{t_i}^{t_{i+1}} \dot{x}_4^2(t)x_4^2(t)dt\\
U_{i3} &= \int_{t_i}^{t_{i+1}} \dot{x}_4^2(t)|\dot{x}_4(t)|dt\\
U_{i4} &= \int_{t_i}^{t_{i+1}} \dot{x}_4^4(t)dt
\end{aligned}$$

The least-square method can be applied to determine the coefficients, α_j, j=0,1,...,4. In fact, the following combination of damping coefficients can be used instead of a general form. Fairly accurate results can be obtained from the following formulae:

Model I: Linear constant plus linear roll

P517434.PDF [Page: 46 of 91]

$$N_\phi = \epsilon_0 + \epsilon_1 |x_4| \tag{4.15}$$

Model II: Linear constant plus quadratic roll

$$N_\phi = \epsilon_0 + \epsilon_1 x_4^2 \tag{4.16}$$

Model IiI: Linear constant plus quadratic roll velocity

$$N_\phi = \epsilon_0 + \epsilon_1 \dot{x}_4^2 \tag{4.17}$$

Model IV: Linear constant plus linear roll velocity

$$N_\phi = \epsilon_0 + \epsilon_1 |\dot{x}_4| \tag{4.18}$$

4.3.2 Estimates of Roll Damping from Empirical Formulae

If there are no roll decay test data available it is assumed that the roll damping coefficient can be computed by

$$N_\phi = \epsilon_0 + \epsilon_1 |x_4| \tag{4.19}$$

The viscous roll damping at a frequency of encounter, ω_e, can be estimated using the work by Schmitke (1978)

$$\lambda_{44}^\nu(\omega_e) = \lambda_{BK}(\omega_e) + \lambda_E(\omega_e) + \lambda_H(\omega_e) + \lambda_F(\omega_e) \tag{4.20}$$

where λ_{BK}, λ_E, λ_H, and λ_F denote the contributions from bilge keel, eddy-making resistance of the hull, hull friction and the viscous effect of appendages other than bilge keel at zero speed, respectively. Each component can be estimated from the empirical formulae given by Schmitke (1978). The coefficients, ϵ_0 and ϵ_1 can be obtained by fitting a set of $\lambda_{44}^\nu(\omega_e)$ vs. ω_e data. The roll damping moment can be expressed as

$$F_4^\nu = \epsilon_0 \dot{x}_4 + \epsilon_1 \dot{x}_4 |x_4| \tag{4.21}$$

P517434.PDF [Page: 47 of 91]

4.4 Other Viscous Forces and Moments

4.4.1 Resistance

The resistance and the cross-flow drag are important to surge, sway and yaw. It is recommended that the resistance model data for the hull be used in the computation. If the test data are not available, empirical formulae may be used for the resistance estimation (see Holtrop and Mennen (1982), for example).

4.4.2 Cross-Flow Drag

The cross-flow drag and moment are calculated by

$$F_2^v(t) = -\frac{1}{2}\rho \int_0^L C_d(x_s)T(x_s)v_2(x_s,t)|v_2(x_s,t)|dx_s \tag{4.22}$$

$$F_6^v(t) = -\frac{1}{2}\rho \int_0^L x_s C_d(x_s)T(x_s)v_2(x_s,t)|v_2(x_s,t)|dx_s \tag{4.23}$$

where $C_d(x_s)$ is the sectional cross-flow drag coefficient; $T(x_s)$ is the local draft of the ship; L is the ship length; $v_2(x_s,t)$ is the transverse relative velocity between the hull and the water particle of the local cross-flow.

4.5 Propeller Thrust

The thrust and torque of the propeller are computed by:

$$F_1^{pt} = (1-t_p)\rho n_p^2 D_p^4 K_T(J) \tag{4.24}$$

and

$$F_4^{pt} = \rho n_p^2 D_p^5 K_Q(J) \tag{4.25}$$

where t_p is the thrust deduction fraction, n_p the revolution per second, D_p the propeller diameter, J the advancing coefficient, K_T the thrust coefficient, and K_Q the torque coefficient. The coefficients t_p, J, K_T, and K_Q can be determined from available propeller charts.

P517434.PDF [Page: 48 of 91]

4.6 Maneuvering Forces

The following nonlinear lateral force and turning moment are adopted in the seakeeping computation (Kijima *et al.*, 1990):

$$\begin{aligned} F_2^m(t) &= \frac{1}{2}\rho L d\tilde{U}^2(Y_\beta\beta' + Y_r r' + Y_{\beta\beta}|\beta'|\beta' \\ &\quad + Y_{rr}|r'|r' + (Y_{\beta\beta r}\beta' + Y_{\beta rr})\beta' r' \end{aligned} \tag{4.26}$$

and

$$\begin{aligned} F_6^m(t) &= \frac{1}{2}\rho L^2 d\tilde{U}^2(N_\beta\beta' + N_r r' + N_{\beta\beta}|\beta'|\beta' \\ &\quad + N_{rr}|r'|r' + (N_{\beta\beta r}\beta' + N_{\beta rr})\beta' r' \end{aligned} \tag{4.27}$$

where L is the ship's length, d is the ship's draft, $\beta' = -u_2/\tilde{U}$ and $r' = \dot{e}_6 L/\tilde{U}$. In the computation, $\tilde{U}$ is the instantaneous forward speed (the ship's mean forward speed plus the surge velocity),and u_2 the instantaneous sway velocity. The hydrodynamic derivatives $Y's$ and $N's$ are determined by empirical formulae or from test results.

4.7 Rudder Forces and Autopilot

The rudder angle δ^r is defined as being positive when turned to port. The normal force acting on the rudder can be evaluated using relations given by Kijima *et al.* (1990):

$$F_N = -\frac{1}{2}\rho\frac{6.13\tilde{\lambda}}{\tilde{\lambda}+2.25}A_r V_r^2 \sin\delta_e^r \tag{4.28}$$

where $\tilde{\lambda}$ is the aspect ratio of the rudder, A_r the rudder planform area, V_r the velocity of the water particle relative to the rudder, and δ_e^r the effective rudder angle:

$$\delta_e^r = \delta^r + \tan^{-1}\frac{u_2 - l_x\dot{e}_6 + l_z\dot{e}_4}{\tilde{U}+u_1} \tag{4.29}$$

Suppose that the normal force acts on the center of pressure C_{rud} of the rudder, the rudder force components can be obtained as follows:

P517434.PDF [Page: 49 of 91]

$$F_1^{rud} = -|F_N| \sin \delta^r \tag{4.30}$$

$$F_2^{rud} = F_N \cos \delta^r \tag{4.31}$$

$$F_4^{rud} = l_z F_N \cos \delta^r \tag{4.32}$$

and

$$F_6^{rud} = -l_x F_N \cos \delta^r \tag{4.33}$$

where l_x and l_z are horizontal and vertical distances between the center of pressure C_{rud} and the center of gravity, respectively; U_{cx} and U_{cy} are the longitudinal and lateral velocity components of current, respectively.

The following autopilot is considered for course-keeping purposes:

$$\delta^r(t) = \begin{cases} \alpha_1^r x_6(t) + \alpha_2^r \dot{x}_6, & \text{if } x_6 > \delta_0^r \\ 0, & \text{if } x_6 \leq \delta_0^r \end{cases} \tag{4.34}$$

where α_1^r is the yaw gain, α_2^r is the yaw rate gain, and δ_0^r is the threshold value of yaw beyond which the rudder is activated.

4.8 Sea Loads

The hydrodynamic sea loads acting on a cross section, x_c, can be expressed as

$$\begin{aligned} F_k^s(t) &= \sum_{j=1}^{6} F_{r_{jk}}^s(t) + F_{d_k}^s(t) + F_{fk_k}^s(t) + F_{rs_k}^s(t) + F_{im_k}^s(t) + F_{im_k}^s(t) \\ &\quad for \quad k = 1, 2, \cdots, 6 \end{aligned} \tag{4.35}$$

where $F_k^s(t)$ are the total sea loads in the kth mode of motion; $F_{r_{jk}}^s(t)$ and $F_{d_k}^s(t)$ are the sea loads due to the radiated and diffracted waves, respectively; $F_{fk_k}^s(t)$ and $F_{rs_k}^s(t)$ are sea loads caused by the incident waves with respect to the Froude-Krylov forces and the restoring forces; $F_{im_k}^S(t)$ are the sea loads of inertial components; and $F_{im_k}^s(t)$ are the sea loads due to the bow-flare impact.

P517434.PDF [Page: 50 of 91]

4.8.1 Sea Loads Due to Radiated and Diffracted Waves

The computations of $F^s_{r_{jk}}(t)$ and $F^s_{d_k}(t)$ are similar to the methods used in computing the radiation and diffraction forces (see Chapter 2). Sea loads are computed as

$$F^s_{r_{jk}}(t) = -\bar{\mu}^f_{jk}\ddot{x}_k(t) - \bar{\lambda}^f_{jk}\dot{x}_k(t) - \bar{\gamma}^f_{jk}x_k(t) - \int_0^t K^s_{r_{jk}}(t-\tau)\dot{x}_k(\tau)d\tau \tag{4.36}$$

where $\bar{\mu}^f_{jk}$, $\bar{\lambda}^f_{jk}$ and $\bar{\gamma}^f_{jk}$ are the time-domain added mass, damping coefficient, and restoring force coefficient of the ship's segment forward of the section x_c, respectively. The superscript f denotes the segment forward of x_c. $K^s_{r_{jk}}(t-\tau)$ is the impulse response function of sea loads due to the ship motions, which can be obtained from

$$\int_0^t K^s_{r_{jk}}(t-\tau)\dot{\xi}_k(\tau)d\tau = \dot{g}^f_{jk}(t) + h^f_{jk}(t) - \bar{\mu}^f_{jk}\ddot{\xi}_k(t) - \bar{\lambda}^f_{jk}\dot{\xi}_k(t) - \bar{\gamma}^f_{jk}\xi_k(t) \tag{4.37}$$

The sea loads due to the diffracted waves are computed from

$$F^s_{d_k} = \int_{-\infty}^{\infty} K^s_{d_k}(t-\tau)\eta_0(\tau)d\tau \tag{4.38}$$

where $K^s_{d_k}(t-\tau)$ denotes the impulse response function of sea loads due to the diffracted waves and $\eta_0(\tau)$ is the wave elevation at the origin of the steady moving coordinate system, and it can be computed from

$$\int_{-\infty}^{\infty} K^s_{d_k}(t-\tau)\bar{\eta}_0(\tau)d\tau = -\dot{g}^f_{j\tau}(t) - h^f_{j\tau}(t) \tag{4.39}$$

4.8.2 Sea Loads Due to Incident Waves

Once the pressure over the panels forward of x_c is determined, sea loads due to the incident waves can be obtained by integrating the pressure over the wetted surface as

$$F^s_{\tau s_k}(t) = \int\int_{S^f_b(t)} \bar{p}^s_I n_k dS \tag{4.40}$$

$$F^s_{fk_k}(t) = \int\int_{S^f_b(t)} \bar{p}^d_I n_k dS \tag{4.41}$$

P5174.34.PDF [Page: 51 of 91]

where $S_b^f(t)$ defines the instantaneous wetted surface forward of x_c.

4.8.3 The Inertial Components of Sea Loads

The inertial shear force and bending moment acting on the section x_c are computed as follows:

$$F_{ins}^s(x_c,t) = m_f(x_c)\ddot{x}_3(t) - m_f(x_c)(x_g^f(x_c) - x_g)\ddot{x}_5(t) \tag{4.42}$$

$$F_{ins}^s(x_c,t) = m_f(x_c)(x_g^f(x_c) - x_c)\ddot{x}_3(t) - m_f(x_c)(x_g^f(x_c) - x_g)(x_g^f(x_c) - x_c)\ddot{x}_5(t) \tag{4.43}$$

where m_f is the mass of a segment of the ship hull between the bow and the cross-section x_c; x_g^f is the x-coordinate of the center of gravity of the ship segment forward of x_c in the ship-fixed coordinate system.

Chapter 5

Variable Hydrodynamic Coefficients

The instantaneous wetted surface changes drastically when a ship travels in large waves. The computation of radiation and diffraction forces in SEALOADS version 1.0 are linearized about the mean wetted surface, which remains time invariant. To extend the version 1.0 code to large waves and steep waves (nonlinear situation), a pseudo-nonlinear model is proposed, where the variable added-mass, damping and restoring coefficients are considered to compute the radiation and diffraction forces.

A position-dependent matrix is set up to consider various attitudes of ship including roll, pitch, heave and their combinations. The hydrodynamic coefficients are pre-computed corresponding to each of these attitudes. When solving equations of ship motion, the instantaneous hydrodynamic coefficients are linearly interpolated from the pre-computed table based on the computed roll, pitch and heave at the previous time step (Ando, 2000). Note that the wetted surface, as defined in Eq.(2.55) for computation of hydrodynamic coefficients, is asymmetric about the centerplane when ship heeled. A literature review on variability of hydrodynamic coefficients was conducted. As an essential tool to set up the position-dependent hydrodynamic coefficient matrix, an automatic panel generator has been developed using NURBS surface based on the work by Danmeier (1999) and Seibert (2000).

5.1 Review of Literature on the Variability of Hydrodynamic Coefficients

One of the earliest studies dealing with dynamic stability conditions of a vessel in time-domain simulation was Elsimillawy and Miller (1986). They used strip theory to obtain the hydrodynamic coefficients such as added mass, inertia and damping. The results showed that variation in draft and angle of heel during ship motions produced large changes in the numerical values of these coefficients. However, because strip theory is linear and the

P517434.PDF [Page: 53 of 91]

longitudinal and lateral modes are uncoupled, questions remained as to the applicability of their results.

More recently, Boyd *et al.* (1995) studied the wave height dependence of the motions of a high speed displacement hull with significant flare and overhang. Using pseudo non-linear strip theory in the frequency domain, and calculating hydrodynamic coefficients at the instantaneous waterline position of the vessel, they determined that the difference between linear and pseudo non-linear predictions was most significant for pitch, particularly for the shallow draft conditions. The non-linear predictions resulted in a reduction in the vessel's response compared with the linear theory for the shallow draft case, and an increase in the predicted response for the deep draft case.

The influence of changing hull attitude on the hydrodynamic coefficients of a trawler form were studied by Conceicao *et al.* (1984). Using strip theory and multiparameter conformal mapping methods they studied the coupled hydrodynamic coefficients of heave, roll, sway of a stationary ship, when the vessel was heeled 5, 10, 15 and 20 degrees. In the upright position, when the hull has port and starboard symmetry, the cross-coupling hydrodynamic coefficients between symmetric (heave, pitch) and antisymmetric (sway, yaw, roll) motions were zero at all frequencies. However, they found that the fluctuations in the hydrodynamic coefficients were not always simply related to heel angle. Finally, the coupled roll, sway and yaw motions may be significantly influenced by the heave and pitch motions.

Using a multiparameter conformal mapping technique, Bishop *et al.* (1980) calculated the two-dimensional sway and roll hydrodynamic coefficients of a variety of symmetric sectional shapes—triangular, rectangular, chine, fine, bulbous. Results show that the coefficients are largest for the triangular section shapes, followed by the rectangular shapes. All coefficients exhibited large changes as a function of frequency.

5.2 An Automatic Panel Generator

In order to set up the position-dependent hydrodynamic coefficient matrix, an automatic panel generator has been developed as an essential tool, using Non-Uniform Rational B-Spline (NURBS) surfaces for geometry representation.

While many mathematical representations, such as cubic polynomials, conformal mapping, have been used to define the hull, NURBS representation has become the preferred method (Rogers and Adams, 1990). It has become popular because it provides a general and flexible description for a large class of free-form geometric shapes. Its intrinsic characteristics of local control, low memory requirements, coupled with a stable and efficient generating algorithm, make it the best choice when describing complicated hull geometries.

P517434.PDF [Page: 54 of 91]

5.2.1 NURBS Representation of Hull Form

A NURBS surface or patch can be defined as follows (Rogers and Adams, 1990):

$$\mathbf{P}(u,v) = \frac{\sum_{i=0}^{n}\sum_{j=0}^{m} w_{ij}\mathbf{C}_{i,j}N_{i,p}(u)N_{j,q}(v)}{\sum_{i=0}^{n}\sum_{j=0}^{m} w_{ij}N_{i,p}(u)N_{j,q}(v)} \tag{5.1}$$

where the surface point $\mathbf{P}(u,v) = (X,Y,Z)$, which can be a input point from offsets, u and v are parametric variables, w_{ij} are the weights, $\mathbf{C}_{i,j}$ form a net of control points, and $N_{i,p}(u)$ and $N_{j,q}(v)$ are the normalized B-splines basis functions of degrees p and q in the u and v directions, respectively. In the program, u is defined along the keel and v is from the bottom to deck. The basis functions can be defined recursively as

$$N_{i,0}(u) = \begin{cases} 1 & \text{if } u_i \le u < u_{i+1} \\ 0 & \text{otherwise} \end{cases} \tag{5.2}$$

$$N_{i,p}(u) = \frac{u - u_i}{u_{i+p} - u_i}N_{i,p-1}(u) + \frac{u_{i+p+1} - u}{u_{i+p+1} - u_{i+1}}N_{i+1,p-1}(u) \tag{5.3}$$

where u_i collectively define the knot vector, $\mathbf{U}$, in the u direction as

$$\mathbf{U} = \{0, 0, ..., 0, u_{p+1}, ..., u_{r-p-1}, 1, 1, ..., 1\} \tag{5.4}$$

Similarly, v_i form a knot vector, $\mathbf{V}$, in the v direction as

$$\mathbf{V} = \{0, 0, ..., 0, v_{q+1}, ..., v_{s-q-1}, 1, 1, ..., 1\} \tag{5.5}$$

The end knots are repeated with multiplicities $p+1$ and $q+1$, respectively, and $r = n+p+1$ and $s = m+q+1$.

As an example, the CPF hull was modeled using NURBS surface with a degree of 3 along u- and v-direction. Figure 5.1 shows the CPF hull surface with the waterplane. The corresponding control net is shown in Figure 5.2, where dashed lines indicate control surface boundaries. Two NURBS patches are used to model the main hull surface and the transom, respectively. The designed waterplane is also presented in Figure 5.1 to show the shallow draft at the stern.

P517434.PDF [Page: 55 of 91]

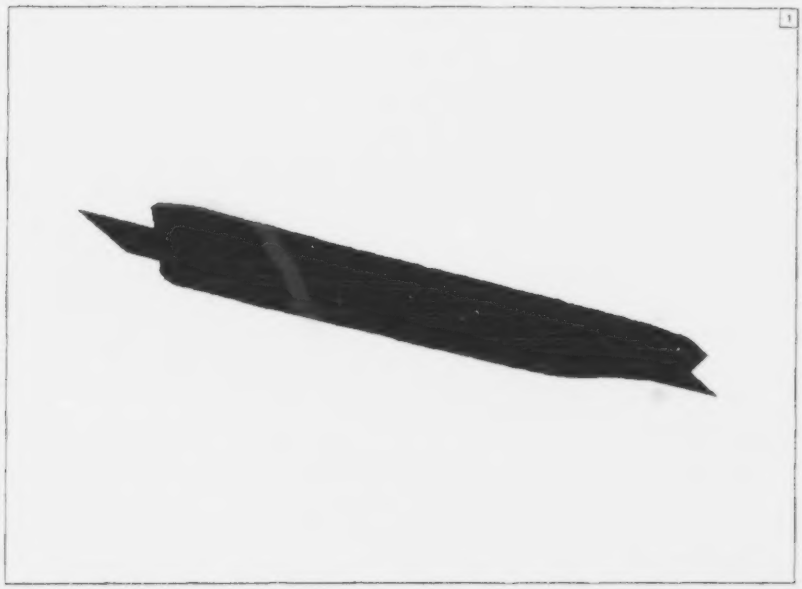

Figure 5.1: Example of mean wetted hull surface and the designed waterplane

5.2.2 Hull Trimming

Having defined the hull by the NURBS surface (the parameterization is shown in Figure 5.3), we now need to determine the surface which lies below the waterline, and to discretize the wetted surface into flat quadrilateral panels. This is accomplished in two steps. First, a surface-surface intersection problem is solved to determine the waterline.

The plane representing the mean water surface can be defined by a point, $\mathbf{P}_0$, and its normal on the surface, $\mathbf{n}$. In parametric space, a point $\mathbf{P}(u, v)$ lies on the intersection of the waterplane and the hull if

$$(\mathbf{P}(u, v) - \mathbf{P}_0) \cdot \mathbf{n} = 0 \tag{5.6}$$

In the current work, we exclude the possibility of pathological hulls producing multiple roots. It is assumed that the waterline crosses the boundaries of the relevant patch at exactly two points.

The contour of the intersection is found by starting at one edge of the uv domain, and marching across to the opposite side. Given a u, Eq.(5.6) can be solved for v using a Newton-Raphson method. This search provides a point (u', v'), such that $F(u', v') < |F_{tol}| = 10^{-5}$, where

P517434 PDF [Page: 56 of 91]

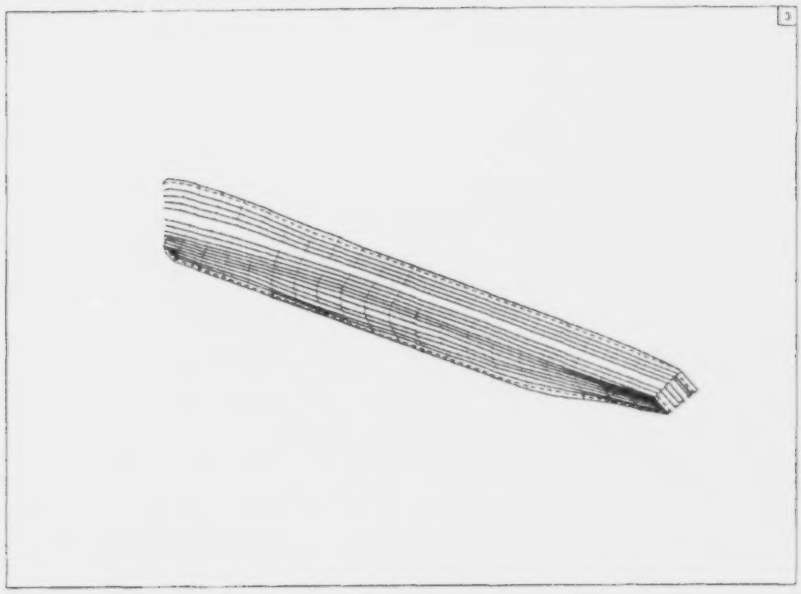

Figure 5.2: Control net

$$F(u', v') = |\mathbf{P}(u', v') - \mathbf{P}_0| \cdot \mathbf{n}, \tag{5.7}$$

and $|F_{tol}|$ is the error tolerance.

If a change, δu, is prescribed in the u-coordinate, we need to search for the appropriate change in v such that $F(u' + \delta u, v' + \delta v) = 0$. The marching algorithm begins by producing a Taylor series expansion of the surface about the point(u', v'), with respect to u and v. Since $F(u', v') \approx 0$, an estimate of δv can be obtained in terms of δu, F_u, and F_v, i.e.

$$\delta v = -\frac{\delta u F_u(u', v')}{F_v(u', v')} \tag{5.8}$$

Given $v_0 = v' + \delta v$ as the initial guess of the waterline's v coordinate, the point $(u' + \delta u, v_0)$ will not lie exactly at the free surface since only linear terms have been retained in the Taylor series. Improvements are then made to v by expanding the surface in v about $(u' + \delta u, v_0)$, where $v_0 = v' + \delta v$ and

$$\delta v = -\frac{F(u' + \delta u, v_0)}{F_v(u' + \delta u, v_0)} \tag{5.9}$$

P517434.PDF [Page: 57 of 91]

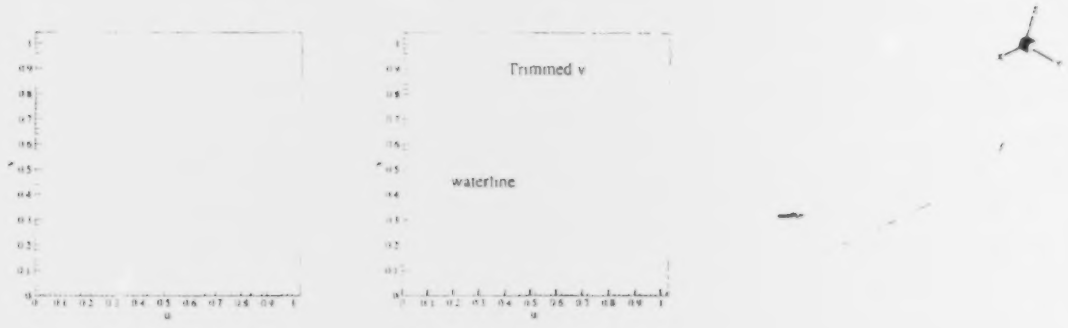

Figure 5.3: Mapping between parametric and physical space

When $F_v(u' + \delta u, v_0)$ is added, the estimate v_0 is improved. This procedure is repeated until $|F(u' + \delta u, v_0)| < F_{tol}$. Because of the quadratic convergence rate of the Newton iteration, an acceptable point is usually found within 4 iterations.

Once the waterline point has been obtained for both port and starboard sides of the hull, the parametric v coordinate can be subdivided into arbitrary pieces before the next u value in the uv plane. This tracing continues until an edge of the uv rectangle of the current patch is reached. The surface trimming process described above repeats for all patches.

In the present program, the uv plane can be subdivided by either constant δu and δv increments, or cosine spacing along the u coordinate.

5.2.3 Panel Generation

As SEALOADS uses constant-source-strength flat panels, the second step is then to transform the $n \times m$ curved mesh into planar panels. Three coordinate systems are used: a reference body coordinate system $(OXYZ)$; a ship-fixed coordinate system $(o_s x_s y_s z_s)$; and a non-Cartesian hull surface coordinate system(ouv).

In the body coordinate, X increases from zero at midships to $L/2$ at the forward perpendicular, where L is the length between perpendiculars. The Y coordinate increases to port from zero at the center plane, and the Z coordinate is positive upwards from zero at the waterplane. The Cartesian point (X, Y, Z) is denoted by the bold face character $\mathbf{X}$. In the ship-fixed coordinate system, the o_s-$x_s y_s$ plane coincides with the waterplane with its normal parallel to $o_s z_s$-axis. The origin o_s is at the point of intersection of mean water surface, the longitudinal plane of symmetry, and the vertical plane passing through midships. The

PS17434.PDF [Page: 58 of 91]

positive x_s-axis points toward the bow and the y_s-axis to the port side.

Let $\mathbf{P}_k = \mathbf{P}_k(u, v), k = 1 \ldots 4$ denote the corner points of a non-planar panel in the reference body coordinate system as shown in Figure 5.4, where $\mathbf{P}_k$'s are determined by the functional relation in Eq.(5.1).

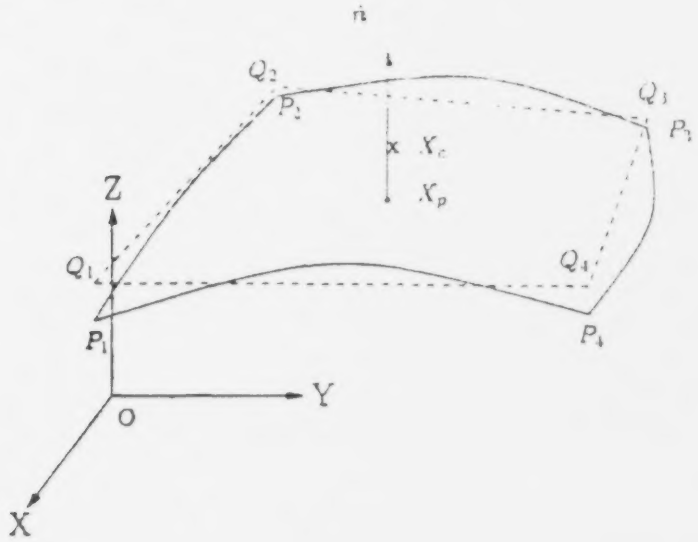

Figure 5.4: Flat Panel Definition

The unit normal to the planar panel is expressed as

$$\hat{\mathbf{n}} = \mathbf{n}/|\mathbf{n}| \tag{5.10}$$

with

$$\mathbf{n} = (\mathbf{P}_4 - \mathbf{P}_2) \times (\mathbf{P}_3 - \mathbf{P}_1) \tag{5.11}$$

By defining a point

$$\mathbf{X}_p = \frac{(\mathbf{P}_1 + \mathbf{P}_2 + \mathbf{P}_3 + \mathbf{P}_4)}{4} \tag{5.12}$$

as the panel definition point, a plane passing through $\mathbf{X}_p$ and having the normal $\hat{\mathbf{n}}$ with the corner points of the plane, $\mathbf{Q}_k$, $k = 1 \ldots 4$ can be obtained by the projection as follows:

P517434.PDF [Page: 59 of 91]

$$\mathbf{Q}_k = \mathbf{P}_k - \hat{\mathbf{n}}[(\mathbf{P}_k - \mathbf{X}_p) \cdot \hat{\mathbf{n}}] \tag{5.13}$$

In SEALOADS, the computation of radiation and diffraction forces are carried out in the ship-fixed coordinate system. Hence, the coordinates computed above in the $OXYZ$ system must be rotated so that their (X, Y, Z) values are relative to the cutting plane. This is accomplished by transformation between $OXYZ$ and $o_s x_s y_s z_s$ as follows:

$$\mathbf{x}_s = [T_x][T_y]\mathbf{X} \tag{5.14}$$

where

$$[T_x] = \begin{bmatrix} 1 & 0 & 0 & 0 \\ 0 & \cos\theta & \sin\theta & 0 \\ 0 & -\sin\theta & \cos\theta & 0 \\ 0 & 0 & 0 & 1 \end{bmatrix} \tag{5.15}$$

and

$$[T_y] = \begin{bmatrix} \cos\phi & 0 & -\sin\phi & 0 \\ 0 & 1 & 0 & 0 \\ \sin\phi & 0 & \cos\phi & 0 \\ 0 & 0 & 0 & 1 \end{bmatrix} \tag{5.16}$$

where θ, ϕ are the rotation angles about the OX and OY axes, respectively. Examples of panelized ship hulls at various positions are given in Appendix G.

P517434.PDF [Page: 60 of 91]

Chapter 6

Concluding Remarks

A computer program, SEALOADS version 1.1, has been developed for computation of ship motions, sea loads and pressure distribution over wetted hull surface in the time domain. The linear model is applied to compute the radiation and diffraction forces. The nonlinear Froude-Krylov forces and restoring forces are computed on the instantaneous wetted surface under the incident wave profile. Viscous damping forces and maneuvering forces are also taken into account. The bow-flare impact forces are computed by a two-dimensional wedge model. As the uniqueness of the code, the impulse response functions are solved by a reliable direct solution approach. A pseudo-nonlinear model has been developed to account for the effect of variable hydrodynamic coefficients. A panel generator based on NURBS surfaces has also been developed as a tool to provide panels for the computation of position-dependent hydrodynamic coefficients. SEALOADS provides a practical means for computing large-amplitude nonlinear loads and motions which are beyond the realm of the conventional linear frequency-domain model.

To obtain a more powerful and reliable tool for predicting ship motions and loads in extreme seas, the following work is recommended:

- Development of a more advanced model for computation of bow-impact forces.
- Application of Stokes wave for the computation of Froude-Krylov forces.
- Improvement of maneuvering/course-keeping module for navy ships.
- Application of the panel-free method for computation of radiation and diffraction forces, in which the exact body geometry will be used and the panelization can be avoided.
- Development of body-exact algorithm for large-amplitude motions to compute radiation and diffraction forces on the instantaneous wetted surface.

- Development of a comprehensive module for hydroelastic response of the ship girder.
- Incorporation of the pre-processors for generating panels and for computing variable hydrodynamic coefficients into the main program SEALOAD for easier and faster execution of the code.

P517434.PDF [Page: 62 of 91]

References

Ando, S. (2000). A Time-Domain Model of Ship Motions and Wave Loads. Oceanic Engineering International, Vol. 4, No. 1, pp. 46-54.

Beck, R. F. and Magee, A. (1990). Time-Domain Analysis for Predicting Ship Motions. Proceedings of IUTAM Symposium, Dynamics of Marine Vehicles and Structures in Waves, London.

Beck, R. F. and King, B. (1989). Time-Domain Analysis of Wave Exciting Forces on Floating Bodies at Zero Forward Speed. Applied Ocean Research, Vol. 11, pp. 19-25.

Beck, R. F. and Liapis, S. J. (1987). Transient Motion of Floating Bodies at Zero Forward Speed. Journal of Ship Research, Vol. 31, pp. 164-176.

Bishop, R.E.D., Price, W.G. and Temarel, P. (1980), Hydrodynamic Coefficients of Some Swaying and Rolling Cylinders of Arbitrary Shape. International Shipbuilding Progress, Vol. 27, pp. 54-65.

Boyd, J., Klaka, K. and Thomas, G. (1995), Analysis of Non-Linear Vessel Motions: Experiments and Predictions. International Conference on Seakeeping and Weather, Proceedings Royal Institute of Naval Architecture, London.

Chang, M. S. (1977). Computation of Three-Dimensional Ship-Motions with Forward Speed. Proceeding Second International Conference on Numerical Ship Hydrodynamics, University of California, Berkeley, pp. 124-135.

Chen, X. B. and Malenica, S. (1996). Uniformly Valid Solution of the Wave-current-body Interaction Problem. 11th International WWWFB, Hamburg, Germany, March 17-20.

Chuang, J. M. (1999). Numerical Computation of Time-Domain Green Function of Free Surface Hydrodynamics. Technical Report Dal-ME-JMC-1999 (Draft), Dalhousie University, Halifax, Nova Scotia, Canada.

Clement, A. H. (1998), An Ordinary Differential Equation for the Green Function of Time-Domain Free-Surface Hydrodynamics. Journal of Engineering Mathematics, Vol. 33, pp. 201-217.

P517454 PDF [Page: 63 of 91]

Conceicao, C.A., Price, W.G. and Temarel, P. (1984), The Influence of Heel on the Hydrodynamic Coefficients of Ship Like Sections and a Trawler Form. International Shipbuilding Progress, Vol. 34, pp. 56-66.

Cong, L., Qiu, W. and Hsiung, C. C. (1999). Theoretical Manual for SEALOADS - A Three-Dimensional Nonlinear Time-Domain Sea Loads Computer Code. DREA Contractor Report CR98-443, Defence Research Establishment Atlantic.

Cummins, W. E. (1962). The Impulse Response Function and Ship Motions, Schiffstechnik, Vol. 9, pp. 101-109.

Danmerer, D.G. (1999). A High-Order Panel Method for Large-Amplitude Simulation of Bodies in Waves. PhD Thesis, Massachusetts Institute of Technology, Cambridge, Massachusetts.

Elsimilawy, N. and Miller, N.S. (1986). Time Simulation of Ship Motions. Transactions SNAME, Vol. 94, pp. 215-240.

Finkelstein, A. (1957). The Initial Value Problem for Transient Water Waves. Communications on Pure and Applied Mathematics, Vol. 10, pp. 511-522.

Guevel, P. and Bougis, J. (1982). Ship Motions with Forward Speed in Infinite Depth. International Shipbuilding Progress, Vol. 29, No. 332, pp. 105-117.

Haddara, M. R. and Bennett, P. (1989). A Study of the Angle Dependence of Roll Damping Moment. Ocean Engineering, Vol. 16, No. 4, pp. 411-427.

Holtrop, J. and Mennen, G. G. J. (1982). An Approximate Power Prediction Method. International Ship Building Progress, No. 335, Vol. 29.

Huang, Y. (1997). Nonlinear Ship Motions by a Rankine Panel Method. PhD dissertation, Department of Ocean Engineering, Massachusetts Institute of Technology.

Huang, Z. J. and Hsiung, C. C. (1993). An Improved 3-D Panel Method to Compute m-terms for Ship Motion. Proceedings of the Second Canadian Marine Dynamics Conference, Vancouver, B.C.

Inglis, R. B. and Price, W. G. (1982). A Three-Dimensional Ship Motion Theory - Comparison between Theoretical Prediction and Experimental Data of the Hydrodynamic Coefficient with Forward Speed. Transactions of Royal Institution of Naval Architects, Vol. 124, pp. 141-157.

Kijima, K., Katsuno, T., Nakiri, Y. and Furukawa, Y. (1990). On the Maneuvering Performance of a Ship with the Parameter of Loading Condition. Journal of the Society of Naval Architects of Japan, Vol. 168, 141-148.

King, B. K., Beck, R. F. and Magee, A.R. (1988). Seakeeping Calculations With Forward

P517434.PDF [Page: 64 of 91]

Speed Using Time Domain Analysis, Proceedings of the Seventeenth Symposium on Naval Hydrodynamics, The Hague, Netherlands.

Liapis, S. and Beck, R. F. (1985). Seakeeping Computations Using Time Domain Analysis. Proceedings of the Fourth International Conference on Numerical Ship Hydrodynamics, Washington, D.C.

Lin, W. M. and Yue, D. K. (1994). Large Amplitude Motions and Wave Loads for Ship Design. Proceedings of the 20th Symposium on Naval Hydrodynamics, Santa Barbra, California.

Lin, W. M. and Yue, D. K. (1990). Numerical Simulations for Large Amplitude Ship Motions in the Time Domain. Proceedings of the 18th Symposium on Naval Hydrodynamics, Ann Arbor, Michigan.

Magee, A. (1994). Seakeeping Applications Using a Time-Domain Method. Proceedings of the 20th Symposium on Naval Hydrodynamics, Santa Barbra, California.

Newman, J. N. (1978). The Theory of Ship Motions. Advances in Applied Mechanics, Vol. 18, pp. 222-283.

Ogilvie, T. F. (1964). Recent Progress toward the Understanding and Prediction of Ship Motions. Proceedings 5th Symposium on Naval Hydrodynamics, ONR, Washington, D.C., pp.3-128

Ogilvie, T. F. (1977). Singularity Perturbation Problem in Ship Hydrodynamics. Advances in Applied Mechanics, Vol. 17, pp. 91-188.

Ogilvie, T. F. and Tuck, E. O. (1969). A Rational Strip Theory of Ship Motion: Part I. Department of Naval Architecture, The University of Michigan, Report No. 013.

Payne, P. R. (1981). The Vertical Impact of a Wedge on a Fluid. Ocean Engineering, Vol. 8, No. 4, pp. 421-436.

Qiu, W., Peng, H. and Hsiung, C. C. (2001). User's Guide for SEALOADS Version 1.1, Technical Report, Martec Limited, Halifax, Nova Scotia, Canada.

Qiu, W. and Hsiung, C. C. (1999). User's Guide for SEALOADS Version 1.0, Technical Report NAP-1999-003, Centre for Marine Vessel Development and Research, Dalhousie University, Halifax, Nova Scotia, Canada.

Qiu, W., Cong, L. and Hsiung, C. C. (1997). Time-domain Slamming Computation. Technical Report, Centre for Marine Vessel Development and Research, Dalhousie University, Halifax, Nova Scotia, Canada.

Rogers, D.F. and Adams, J.A. (1990). Mathematical elements for computer graphics. McGraw-Hill Inc., New York, 2nd Edition.

P517434.PDF [Page: 65 of 91]

Seibert, G. (2000). The Influence of Variable Added Mass and Damping in a Three-Dimensional Time Domain Ship Motion Program. Master's Thesis, Dalhousie University, Halifax, Nova Scotia, Canada.

Schmitke, R. T. (1978). Ship Sway, Roll and Yaw Motion in Oblique Seas. Transactions SNAME, Vol. 86.

Stoker, J. J. (1957). Water Wave. International Science Publishers, Inc., New York.

van Oortmerssen, Gerard (1976). The Motion of a Moored Ship in Waves. NSMB Publication No. 510.

Wehausen, J. V. (1967). Initial Value Problem for the Motion in an Undulating Sea of a Body with Fixed Equilibrium Position. Journal of Engineering Mathematics, Vol. 1, pp. 1-19.

Wehausen, J. V. (1971). The Motion of Floating Bodies. Annual Review of Fluid Mechanics, Vol. 3, pp. 237-268.

Wehausen, J. V. and Laitone, E. V. (1960). Surface Waves. Handbuch der Physik, Springer-Verlag, Vol. 9.

P517434.PDF [Page: 66 of 91]

Appendix A

Analytical Solution of the Time-Dependant Green Function

The oscillatory part of the time-dependent Green function $F(P,Q;t-\tau)$ given by Eq.(2.32) can be analytically solved using an ordinary differential equation derived by Clement (1998).

Equation (2.32) is rewritten as

$$\bar{F}(\bar{r},\bar{Z};t-\tau) = 2\int_0^\infty \sqrt{gk}\sin[\sqrt{gk}(t-\tau)e^{k(\bar{z}+\bar{z}')}J_0(k\bar{R})dk \tag{A.1}$$

where $\bar{Z} = \bar{z} + \bar{z}'$. Introducing

$$\begin{aligned} K &= gk \\ z+z' &= \frac{\bar{z}+\bar{z}'}{g} \\ R &= \frac{\bar{R}}{g} \\ z &= \frac{\bar{z}}{g} \\ F(r,Z;t-\tau) &= g\bar{F}(\bar{r},\bar{Z};t-\tau) \end{aligned} \tag{A.2}$$

leads to

$$F(r,Z;t-\tau) = 2\int_0^\infty \sqrt{K}\sin[\sqrt{K}(t-\tau)]e^{K(z+z')}J_0(KR)dK \tag{A.3}$$

By a simple change of variable ($KR_1 \rightarrow \lambda$) in (A.3), the memory part of the time-dependent Green function can be expressed as a function of two real variables (μ,τ):

P517434.PDF [Page: 67 of 91]

$$F(r, Z; t) = 2R_1^{-3/2}\tilde{F}(\mu, \tau) \tag{A.4}$$

with

$$\tilde{F}(\mu, \tau) = \int_0^\infty J_0(\lambda\sqrt{1-\mu^2})e^{-\lambda\mu}\sqrt{\lambda}\sin(\sqrt{\lambda}\tau)d\lambda \tag{A.5}$$

where $\mu = -Z/R_1$ and $\tau = t\sqrt{R_1}$. $\tilde{F}(\mu, \tau)$ satisfies the following fourth-order differential equation

$$\tilde{F}^{(4)} + \mu\tau\tilde{F}^{(3)} + (\frac{1}{4}\tau^2 + 4\tau)\tilde{F}^{(2)} + \frac{7}{4}\tau\tilde{F}^{(1)} + \frac{9}{4}\tilde{F} = 0 \tag{A.6}$$

with the initial conditions

$$\tilde{F}^{(2k)}(\mu, 0) = 0, \quad \tilde{F}^{(2k+1)}(\mu, 0) = (-1)^k(k+1)!P_{k+1}(\mu); \quad k = 0, 1, \ldots \tag{A.7}$$

where $\tilde{F}^{(k)}$ denotes the kth-order differenciation of $\tilde{F}$ with τ.

The derivatives of the Green function, $\partial F/\partial x$ and $\partial F/\partial y$ can be obtained from

$$\frac{\partial F}{\partial x} = \frac{x - x'}{r}F_r \tag{A.8}$$

$$\frac{\partial F}{\partial y} = \frac{y - y'}{r}F_r \tag{A.9}$$

and

$$F_r(r, Z; t) = -2R_1^{-5/2}K(\mu, \tau) \tag{A.10}$$

where $K(\mu, \tau)$ satisfies the fourth-order differential equation:

$$K^{(4)} + \mu\tau K^{(3)} + (\frac{1}{4}\tau^2 + 6\tau)K^{(2)} + \frac{11}{4}\tau K^{(1)} + \frac{21}{4}K = 0 \tag{A.11}$$

with the initial conditions

$$K^{(2k)}(\mu, 0) = 0, \quad K^{(2k+1)}(\mu, 0) = (-1)^k(k+1)!\sqrt{1-\mu^2}\frac{d}{d\mu}P_{k+2}(\mu); \quad k = 0, 1, \ldots \tag{A.12}$$

P517434.PDF [Page: 68 of 91]

Equations (A.6) and (A.11) can be written in a general form:

$$K_F^{(4)} + \mu\tau K_F^{(3)} + (\frac{1}{4}\tau^2 + A\tau)K_F^{(2)} + B\tau K_F^{(1)} + CK_F = 0 \tag{A.13}$$

where

$$\begin{aligned} A = 4;\ \ B = \frac{7}{4};\ \ C = \frac{9}{4} \quad &\text{for} \quad K_F = \tilde{F} \\ A = 6;\ \ B = \frac{11}{4};\ \ C = \frac{21}{4} \quad &\text{for} \quad K_F = K \end{aligned} \tag{A.14}$$

Now, we can obtain the time-domain Green's function and its derivatives by solving the fourth-order ordinary differential equation (A.13). This equation can be solved by using a Runge-Kutta scheme (Clement, 1998). Here, a series expansion method is applied to achieve an analytical solution (Chuang, 1999).

Assuming

$$K_F(t) = a_0 + \sum_{n=1}^{\infty} a_n (t - t_1)^n \tag{A.15}$$

where t_1 is the initial time, then the derivatives of $K_F(t)$ are

$$\begin{aligned} K_F^{(1)}(t) &= a_1 + \sum_{n=2}^{\infty} n a_n (t - t_1)^{n-1} \\ K_F^{(2)}(t) &= 2a_2 + \sum_{n=3}^{\infty} n(n-1) a_n (t - t_1)^{n-2} \\ K_F^{(3)}(t) &= 6a_3 + \sum_{n=4}^{\infty} n(n-1)(n-2) a_n (t - t_1)^{n-3} \\ K_F^{(4)}(t) &= 24a_4 + \sum_{n=5}^{\infty} n(n-1)(n-2)(n-3) a_n (t - t_1)^{n-4} \end{aligned} \tag{A.16}$$

If we rewrite the initial conditions as

$$K_F^{(1)}(t_1) = d_0^0,\ \ K_F^{(2)}(t_1) = d_1^0,\ \ K_F^{(3)}(t_1) = d_2^0,\ \ K_F^{(4)}(t_1) = d_3^0 \tag{A.17}$$

then

$$a_0 = d_0^0, \quad a_1 = d_1^0, \quad a_2 = d_2^0, \quad a_3 = d_3^0 \tag{A.18}$$

By defining

$$\begin{array}{lll} \kappa_1 = 1, & \kappa_2 = \mu, & \kappa_3 = -\mu t_1 \\ \kappa_4 = \frac{1}{4}, & \kappa_5 = \frac{1}{2}t_1, & \kappa_6 = -\frac{1}{4}t_1^2 + A\mu \\ \kappa_7 = B, & \kappa_8 = Bt_1, & \kappa_9 = C \end{array} \tag{A.19}$$

Equation(A.13) can be written as

$$\begin{aligned} &\kappa_1 K_F^{(4)} + \kappa_2(t-t_1)K_F^{(3)} + \kappa_3 K_F^{(3)} + \kappa_4(t-t_1)^2 K_F^{(2)} + \\ &\kappa_5(t-t_1)K_F^{(2)} + \kappa_6 K_F^{(2)} + \kappa_7(t-t_1)K_F^{(1)} + \kappa_8 K_F^{(1)} + \kappa_9 K_F = 0 \end{aligned} \tag{A.20}$$

Substituting Eq.(A.17) into Eq.(A.21) leads to

$$\sum_{i=0}^{9} C_i = 0 \tag{A.21}$$

where

$$\begin{aligned} C_1 &= 24\kappa_1 a_4 + \sum_{n=1}^{\infty} x_1(n+4)(n+3)(n+2)(n+1)a_{n+4}(t-t_1)^n \\ C_2 &= \sum_{n=1}^{\infty} \kappa_2(n+2)(n+1)na_{n+2}(t-t_1)^n \\ C_3 &= 6\kappa_3 a_3 + \sum_{n=1}^{\infty} \kappa_3(n+3)(n+2)(n+1)a_{n+3}(t-t_1)^n \\ C_4 &= \sum_{n=1}^{\infty} \kappa_4 nn(-1)a_n(t-t_1)^n \\ C_5 &= \sum_{n=1}^{\infty} \kappa_5(n+1)na_{n+1}(t-t_1)^n \\ C_6 &= 2\kappa_6 a_2 + \sum_{n=1}^{\infty} \kappa_6(n+2)(n+1)a_{n+2}(t-t_1)^n \end{aligned} \tag{A.22}$$

P517434 PDF [Page: 70 of 91]

$$C_7 = \sum_{n=1}^{\infty} \kappa_7 n a_n (t - t_1)^n$$

$$C_8 = \kappa_8 a_1 + \sum_{n=1}^{\infty} \kappa_8 (n+1) a_{n+1} (t - t_1)^n$$

$$C_9 = \kappa_6 a_0 + \sum_{n=1}^{\infty} \kappa_9 a_n (t - t_1)^n$$

Once the coefficients of the series are obtained from (A.21), then we can solve for $\tilde{F}(\mu, \tau)$ and $K(\mu, \tau)$. The vertical derivative can be computed from

$$\frac{\partial F}{\partial z} = \frac{\partial F}{\partial Z} = -\frac{\partial^2 F}{\partial t^2} \tag{A.23}$$

The Green function, $F(\mu, \tau)$ and its derivatives denoted as $F_t(\mu, \tau)$, $F_x(\mu, \tau)$, $F_y(\mu, \tau)$ and $F_z(\mu, \tau)$ are plotted in Figure A.1, where the upper bound for $F(\mu, \tau)$ is plotted as a black straight line.

P517434 PDF [Page: 71 of 91]

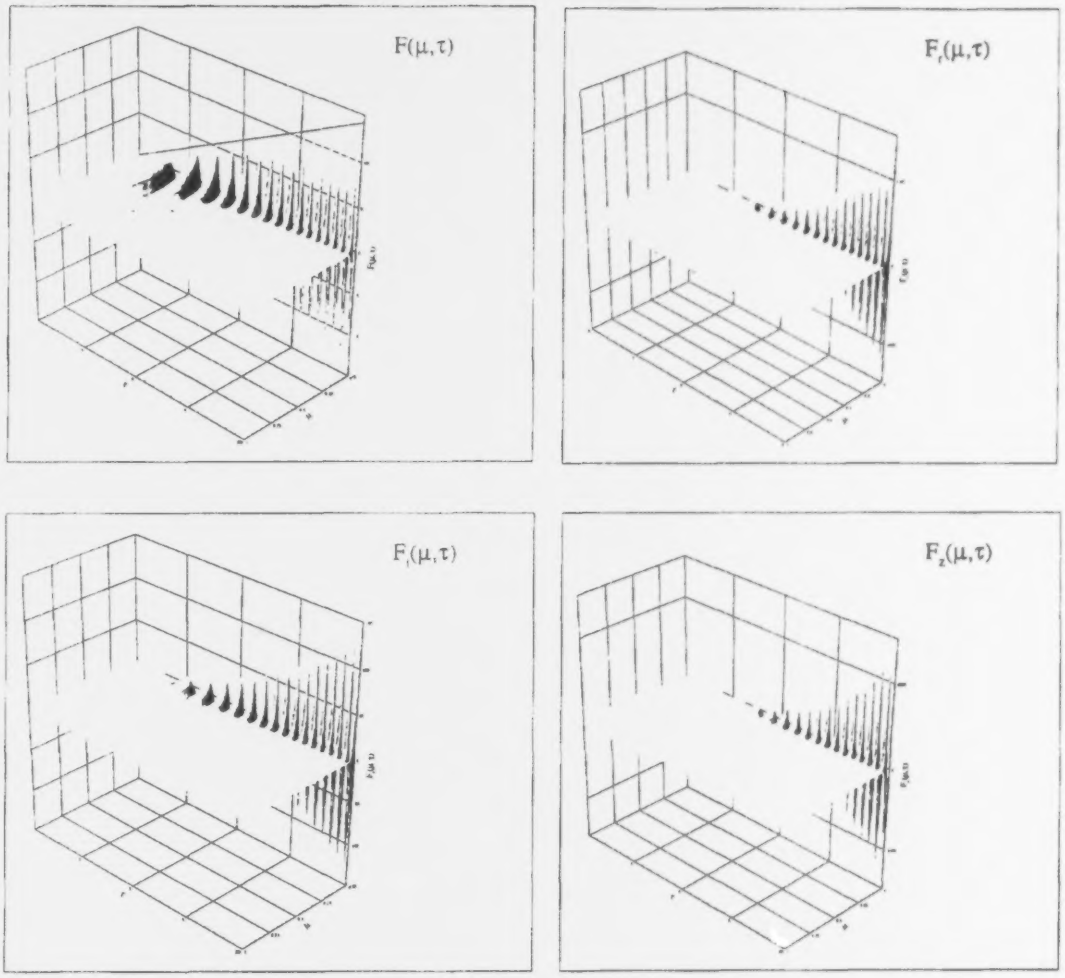

Figure A.1: The Green function and its derivatives in its natural variables (μ,τ)

P517434.PDF [Page 52 of 91]

Appendix B

Numerical Solution of the Source Strength from the Integral Equation

The boundary integral equation

$$\frac{\partial\phi(P;t)}{\partial n} = -\frac{1}{2}\sigma(P;t) - \frac{1}{4\pi}\int_0^t d\tau \int\int_{\bar{S}_b} \frac{\partial G(P,Q;t-\tau)}{\partial n}\sigma(Q;\tau)dS - \frac{U_0^2}{4\pi g}\int_0^t d\tau \oint_\Gamma n_1 \frac{\partial G(P,Q;t-\tau)}{\partial n}\sigma(Q;\tau)dl \tag{B.1}$$

Assuming that the source strength is constant over a panel, this equation can be written in the discretized form by using the trapezoidal integration scheme,

$$-\frac{1}{2}\boldsymbol{\sigma}_i^{k_t} - \sum_{j=1}^{n}\boldsymbol{\sigma}_i^{k_t}\mathbf{I}_{ij}^0 + \Delta t[\frac{1}{2}\sum_{j=1}^{n}\boldsymbol{\sigma}_j^0\mathbf{I}_{Fij}^{k_t} + \sum_{k=1}^{k_t-1}\sum_{j=1}^{n}\boldsymbol{\sigma}_j^k\mathbf{I}_{Fij}^{k_t-k}] + \Delta t[\frac{1}{2}\sum_{j=1}^{m}(\boldsymbol{\sigma}_L)_j^0\mathbf{L}_{Fij}^{k_t} + \sum_{k=1}^{k_t-1}\sum_{j=1}^{m}(\boldsymbol{\sigma}_L)_j^k\mathbf{L}_{Fij}^{k_t-k}] = (\mathbf{V}_n)_i^{k_t} \tag{B.2}$$

where i indicates a field point and j indicates a source point; n and m are the number of panels and segments on the waterline, respectively; $\boldsymbol{\sigma}_i^{k_t}$ are the source strengths in six modes of panel i at time step k_t; $\mathbf{V}_n$ is the normal velocities in six modes; $(\boldsymbol{\sigma}_L)_j^{k_t}$ denotes the source strength on waterline segment j at time step k_t; and

$$\mathbf{I}_{ij}^0 = -\frac{1}{4\pi}\iint_{\bar{S}_{b_j}}(\frac{\partial G_0}{\partial n})_{ij}dS \tag{B.3}$$

P517434.PDF [Page 73 of 91]

$$\mathbf{I}_{Fij}^{k_t-k} = -\frac{1}{4\pi}\iint_{S_{b_j}} (\frac{\partial F}{\partial n})_{ij}^{k_t-k} dS \tag{B.4}$$

$$\mathbf{L}_{Fij}^{k_t-k} = -\frac{U^2}{4\pi g}\int_{L_j} (n_1)_j (\frac{\partial F}{\partial n})_{ij}^{k_t-k} dL \tag{B.5}$$

With these definitions, we obtain a system of linear equations which are solved for $\boldsymbol{\sigma}_j^{k_t}$,

$$\sum_{j=1}^{n} \mathbf{A}_{ij}^{k_t} \boldsymbol{\sigma}_j^{k_t} = \mathbf{B}_i^{k_t} \qquad i = 1, 2, \cdots n \tag{B.6}$$

where

$$\mathbf{A}_{ij}^{k_t} = -\frac{1}{2}\delta(i,j) + \mathbf{I}_{ij}^{0} \tag{B.7}$$

and

$$\begin{aligned} \mathbf{B}_i^{k_t} \;=\; & (\mathbf{V}_n)_i^{k_t} - \Delta t[\frac{1}{2}\sum_{j=1}^{n} \boldsymbol{\sigma}_j^0 \mathbf{I}_{Fij}^{k_t} + \sum_{k=1}^{k_t-1}\sum_{j=1}^{n} \boldsymbol{\sigma}_j^k \mathbf{I}_{Fij}^{k_t-k}] \\ & -\Delta t[\frac{1}{2}\sum_{j=1}^{m} (\boldsymbol{\sigma}_L)_j^0 \mathbf{L}_{Fij}^{k_t} + \sum_{k=1}^{k_t-1}\sum_{j=1}^{m} (\boldsymbol{\sigma}_L)_j^k \mathbf{L}_{Fij}^{k_t-k}] \end{aligned} \tag{B.8}$$

P517434.PDF [Page: 74 of 91]

Appendix C

Computation of m-terms

The steady flow effect on the radiation wave problem is shown by the body boundary condition which is represented by m-terms, given in (2.23) and (2.24) as

$$\begin{aligned}(m_1, m_2, m_3) &= -(\mathbf{n}\cdot\nabla)\nabla\Phi^{db} \\ &= -(n_1\Phi^{db}_{xx} + n_2\Phi^{db}_{xy} + n_3\Phi^{db}_{xz},\ n_1\Phi^{db}_{yx} + n_2\Phi^{db}_{yy} + n_3\Phi^{db}_{yz}, \\ &\quad n_1\Phi^{db}_{zx} + n_2\Phi^{db}_{zy} + n_3\Phi^{db}_{zz})\end{aligned}$$

$$\begin{aligned}(m_4, m_5, m_6) &= \mathbf{r}_g \times (m_1, m_2, m_3) - \mathbf{n}\times\nabla\Phi^{db} \\ &= \mathbf{r}_g \times (m_1, m_2, m_3) + (n_3\Phi^{db}_{y} - n_2\Phi^{db}_{z},\ n_1\Phi^{db}_{z} - n_3\Phi^{db}_{x}, \\ &\quad n_2\Phi^{db}_{x} - n_1\Phi^{db}_{y})\end{aligned}$$

Since the source strength is assumed to be constant over a panel, it makes the computation of the second-order derivatives of the potential difficult. In the current work, a scheme proposed by Chen and Malenica (1996) is used to compute the derivatives and m-terms. Unlike the scheme used by Huang and Hsiung(1993), the second-order derivatives can also be computed individually by the scheme of Chen and Malenica (1996).

The velocities can be expressed as

$$\frac{\partial\phi^{db}}{\partial x} = \int\int_{\bar{S}_b} \sigma_x G_0 dS \tag{C.1}$$

$$\frac{\partial\phi^{db}}{\partial y} = \int\int_{\bar{S}_b} \sigma_y G_0 dS \tag{C.2}$$

$$\frac{\partial \phi^{db}}{\partial z} = \int\int_{\hat{S}_b} \sigma_z G_0 dS \tag{C.3}$$

where σ_x, σ_y and σ_z are source strengths; Since the velocities are known, the source strengths can be solved from the above equations. The second-order derivatives of the potential can be obtained as

$$\frac{\partial^2 \phi^{db}}{\partial x^2} = \int\int_{\hat{S}_b} \sigma_x \frac{\partial G_0}{\partial x} dS \tag{C.4}$$

$$\frac{\partial^2 \phi^{db}}{\partial x \partial y} = \int\int_{\hat{S}_b} \sigma_x \frac{\partial G_0}{\partial y} dS \tag{C.5}$$

$$\frac{\partial^2 \phi^{db}}{\partial x \partial z} = \int\int_{\hat{S}_b} \sigma_x \frac{\partial G_0}{\partial z} dS \tag{C.6}$$

$$\frac{\partial^2 \phi^{db}}{\partial y^2} = \int\int_{\hat{S}_b} \sigma_y \frac{\partial G_0}{\partial y} dS \tag{C.7}$$

$$\frac{\partial^2 \phi^{db}}{\partial y \partial z} = \int\int_{\hat{S}_b} \sigma_y \frac{\partial G_0}{\partial z} dS \tag{C.8}$$

and

$$\frac{\partial^2 \phi^{db}}{\partial z^2} = -\frac{\partial^2 \phi^{db}}{\partial x^2} - \frac{\partial^2 \phi^{db}}{\partial x^2} \tag{C.9}$$

Substituting equations (C.4) to (C.9) into (2.23) and (2.24), the m-terms can be obtained.

P517434.PDF [Page: 76 of 91]

Appendix D

Numerical Solution of the Impulse Response Function

As shown in equations (2.62), (2.63), (2.68) and (2.66), the impulse response functions can be solved from the Fredholm integral equation of the first kind. Here, we define a general equation

$$F_r(t) = \int_{t_1}^{t_2} K_r(t-\tau)\eta_I d\tau \tag{D.1}$$

where

$F_r(t) = \dot{g}_{jk}(t) + h_{jk}(t) - \bar{\mu}_{jk}\ddot{\xi}_k(t) - \bar{\lambda}_{jk}\dot{\xi}_k(t) - \bar{\gamma}_{jk}\xi_k(t)$ for the radiation force,
$F_r(t) = -\dot{g}_{j7}(t) - h_{j7}(t)$ for the diffraction force,
$F_r(t) = p_k^R(x,y,z;t)$ for the radiation pressure,
$F_r(t) = p_D(x,y,z;t)$ for the diffraction pressure;

and

$K_r = K_{p_k}^R(x,y,z;t)$, $\eta_I = \dot{\xi}_k(t)$, $t_1 = 0$, $t_2 = t$ for the radiation problem,
$K_r = K_p^D(x,y,z;t)$, $\eta_I = \bar{\eta}_0(t)$, $t_1 = -\infty$, $t_2 = \infty$ for the diffraction problem.

Equation(D.1) can be solved by the direct solution scheme (Cong *et al.*, 1999). The convolution equation can be discretized as

$$F_{r_m} = \sum_{n=1}^{m-1} K_{r_{m-n}}\eta_{I_n}\Delta t + \frac{1}{2}[K_{r_m}\eta_{r_0} + K_{r_0}\eta_{I_m}]\Delta t \quad m = 1, 2, ..., M \tag{D.2}$$

where M is the total number of steps defined by $t_M = M\Delta t$. With simplified notations,

P517434.PDF [Page: 77 of 91]

$$\begin{cases} a_m &= \eta_{r_m} \\ x_m &= K_{r_m} \\ b_m &= F_{r_m} \end{cases}$$

Equation (D.2) becomes a system of equations in terms of x_m,

$$\begin{cases} \frac{1}{2}a_1 x_0 + \frac{1}{2}a_0 x_1 & & & & & = \frac{b_1}{\Delta t} \\ \frac{1}{2}a_2 x_0 + a_1 x_1 + \frac{1}{2}a_0 x_2 & & & & & = \frac{b_2}{\Delta t} \\ \cdots & & & & & = \cdots \\ \frac{1}{2}a_M x_0 + a_{M-1} x_1 + \cdots + a_1 x_{M-1} + \frac{1}{2}a_0 x_M & & & & & = \frac{b_M}{\Delta t} \end{cases} \tag{D.3}$$

It is evident that the systems of equations (D.3) are indeterminate, because the total number of unknowns M is larger than the total number of equations by 1. An additional physical condition has to be provided to make (D.3) closed. When time $t_m = m\Delta t$ is sufficiently long, the response function K_{r_m} becomes quite smooth and goes to zero uniformly, i.e, the first-order time derivative of K_{r_m} tends to zero. An additional condition for K_{r_m} at a specific time instant can be obtained by approximating the time derivative with a third-order finite difference, as follows:

$$x_{N-4} - 3x_{N-3} + 3x_{N-2} + x_{N-1} = 0, \quad \text{for} \quad N = M + 1 \tag{D.4}$$

P517434.PDF [Page: 78 of 91]

Appendix E

Pressure over a Panel due to Incident Waves

When computing the hydrodynamic pressure due to incident waves, it is assumed that the pressure is linearly distributed over a panel. The hull is discretized by quadrilateral panels. A quadrilateral panel is shown in Fig. E-1.

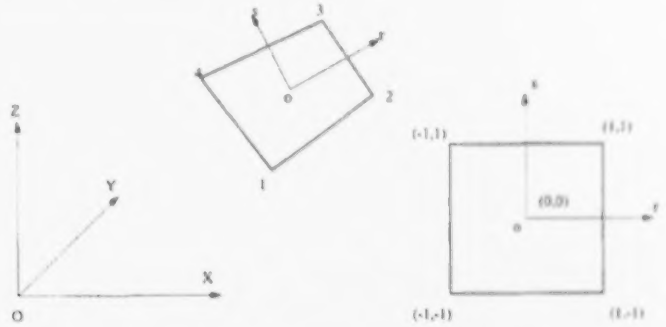

Figure E.1: A quadrilateral panel and the local reference frame

The pressure at any point on a panel due to the incident wave is given by Eq.(4.3) as

$$\bar{p}_I(X,Y,Z;t) = \sum_{i=1}^{4} N_i(X,Y,Z) p_{I_i}(X,Y,Z) \tag{E.1}$$

The shape function $N_i(r,s)$ in the local reference frame $or\,s$ can be expressed as

PS17434.PDF [Page: 79 of 91]

$$
\begin{aligned}
N_1 &= \frac{1}{4}(1-r)(1-s) \\
N_2 &= \frac{1}{4}(1+r)(1-s) \\
N_3 &= \frac{1}{4}(1+r)(1+s) \\
N_4 &= \frac{1}{4}(1-r)(1+s)
\end{aligned}
$$

and $r, s \in [-1, 1]$. The pressure at a local coordinates (r, s), is then written as

$$\bar{p}_I(r, s; t) = \sum_{i=1}^{4} N_i(r, s) p_{I_i} \tag{E.2}$$

The Froude-Krylov force, for example, may be obtained as

$$F_k^{fk}(t) = -\sum_{i=1}^{m}\sum_{j=1}^{n} w_i w_j p_I^d(r_i, s_j) n_k(r_i, s_j) |J(r_i, s_j)| \tag{E.3}$$

where w_i and w_j are the weighting factors at (r_i, s_j), and $|J(r_i, s_j)|$ is the Jacobian.

P517434.PDF [Page: 80 of 91]

Appendix F

Structure of SEALOADS Version 1.1 Code

The computer program, SEALOADS Version 1.1, for prediction of nonlinear motions, pressure distribution, and sea loads on a ship hull in large waves, consists of four main modules:

(1) radiation module,

(2) diffraction module,

(3) damping module, and

(4) motion, pressure and sea loads module.

The radiation module depends on the forward speed. The impulse response functions for the radiation forces, sea loads, and the pressures on each panel are solved in this module. The diffraction module depends on the forward speed and the wave heading. The impulse response functions for the diffraction forces, sea loads, and the pressures on each panel are solved in this module. Based on the outputs from these two modules, and the damping coefficients from the damping module, the ship motion and pressure distribution and sea loads can be computed for the various wave heights in regular and irregular waves. The code structures for SEALOADS Version 1.1 is shown in Figures F.1 to F.4.

P517434.PDF [Page: 81 of 91]

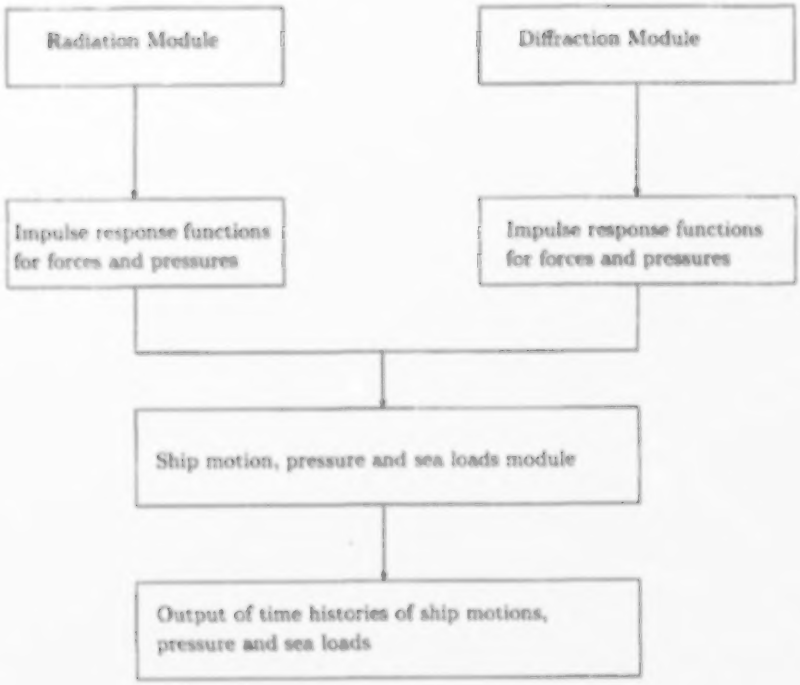
Radiation Module
Diffraction Module
Impulse response functions for forces and pressures
Impulse response functions for forces and pressures
Ship motion, pressure and sea loads module
Output of time histories of ship motions, pressure and sea loads

Figure F.1: Code structure of SEALOADS Version 1.1

P517434.PDF [Page: 82 of 91]

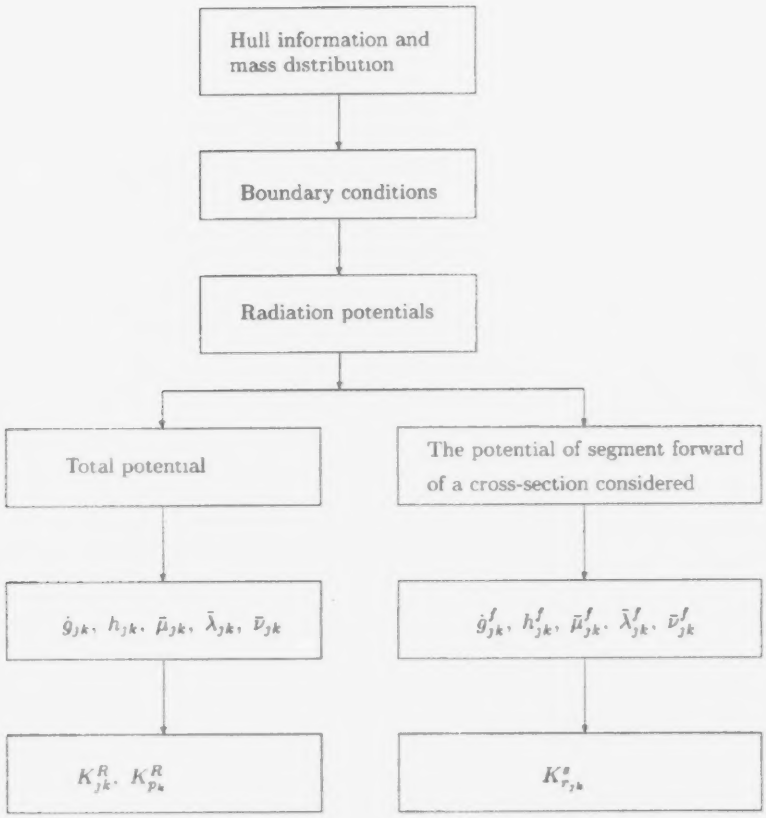

Figure F.2: Code structure of Radiation Module

PS17434.PDF [Page: 83 of 91]

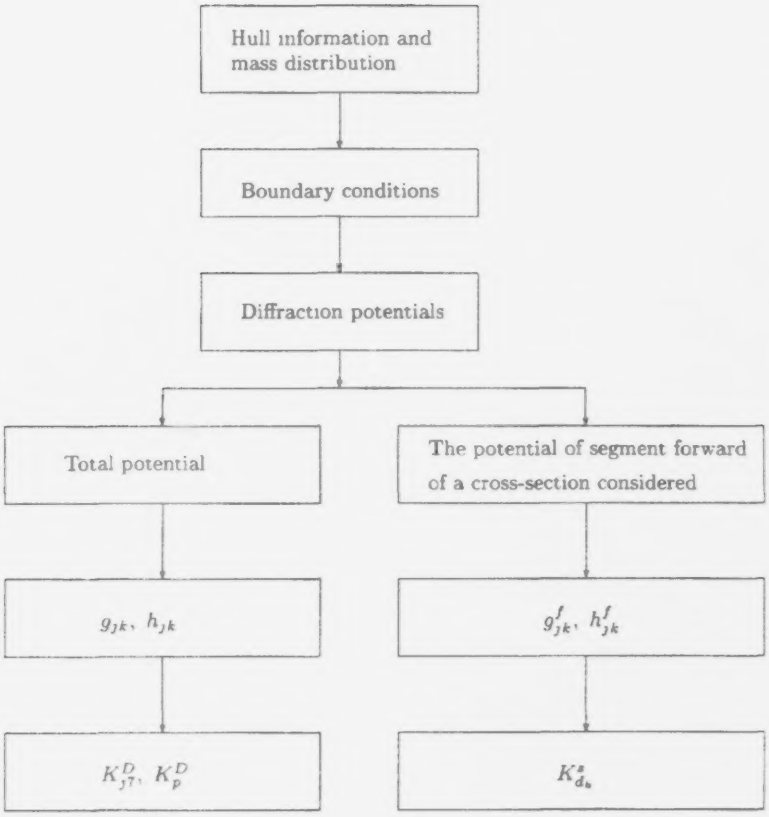

Figure F.3: Code structure of Diffraction Module

P517434 PDF [Page: 84 of 91]

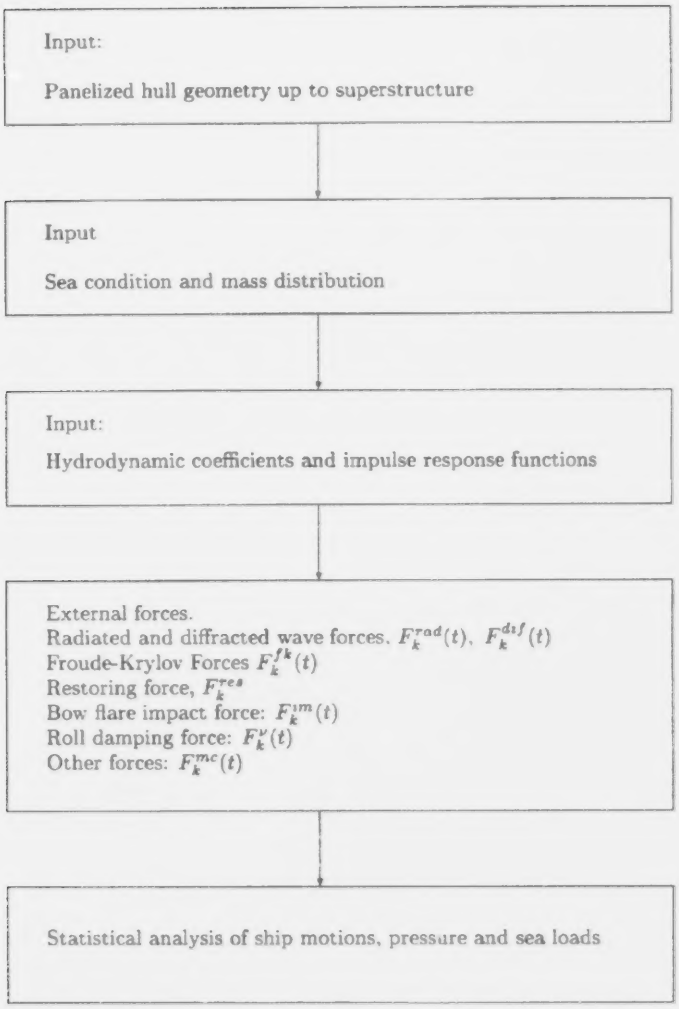
Input:
Panelized hull geometry up to superstructure
Input
Sea condition and mass distribution
Input:
Hydrodynamic coefficients and impulse response functions
External forces.
Radiated and diffracted wave forces, $F_k^{rad}(t)$, $F_k^{dif}(t)$
Froude-Krylov Forces $F_k^{fk}(t)$
Restoring force, F_k^{res}
Bow flare impact force: $F_k^{im}(t)$
Roll damping force: $F_k^{v}(t)$
Other forces: $F_k^{mc}(t)$
Statistical analysis of ship motions, pressure and sea loads

Figure F.4: Code structure of Ship Motion, Pressure and Sea Loads Module

P517434.PDF [Page: 85 of 91]

Appendix G

Examples of Panelized Hull

Figures G.1, G.2 and G.3 show three panelized ship hulls at three positions. These figures also demonstrate the drastically changed wetted surface.

P517434.PDF [Page: 86 of 91]

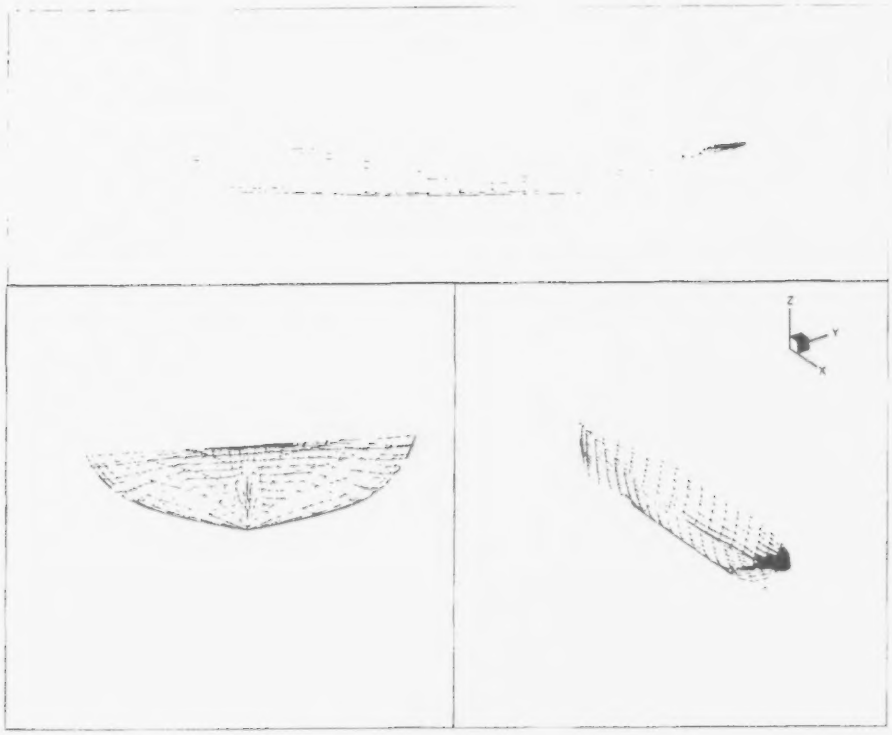

Figure G.1: A CPF Hull heeled by port side 2.5°, trimmed 0° and heaved 2.0m

P517434.PDF [Page: 87 of 91]

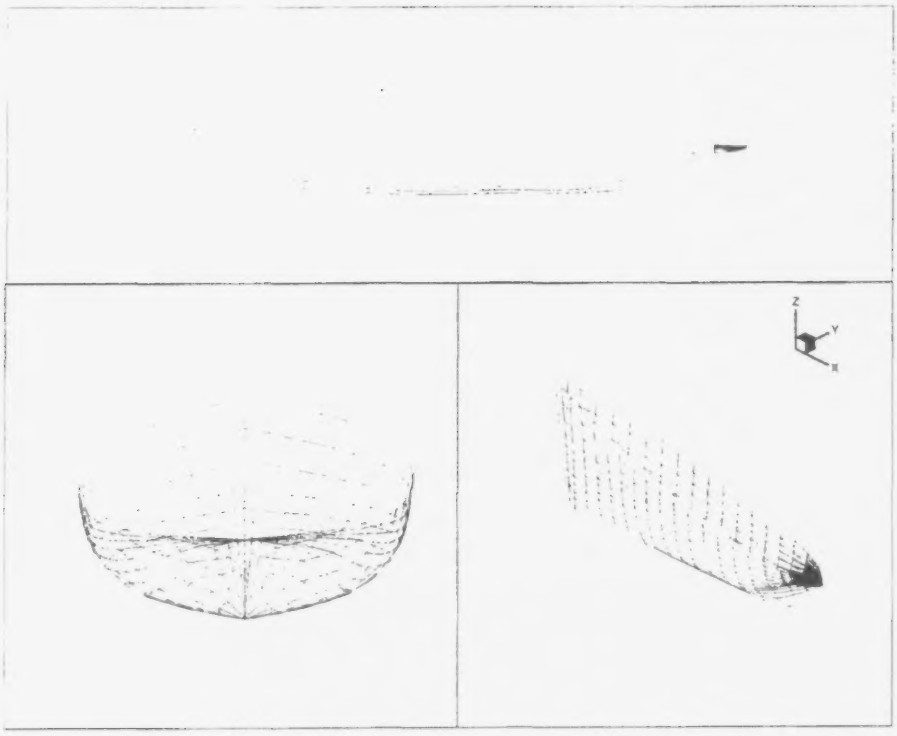

Figure G.2: A CPF Hull heeled by port side 1.5°, trimmed by bow 2.5° and heaved 0.0m

P517434.PDF [Page: 88 of 91]

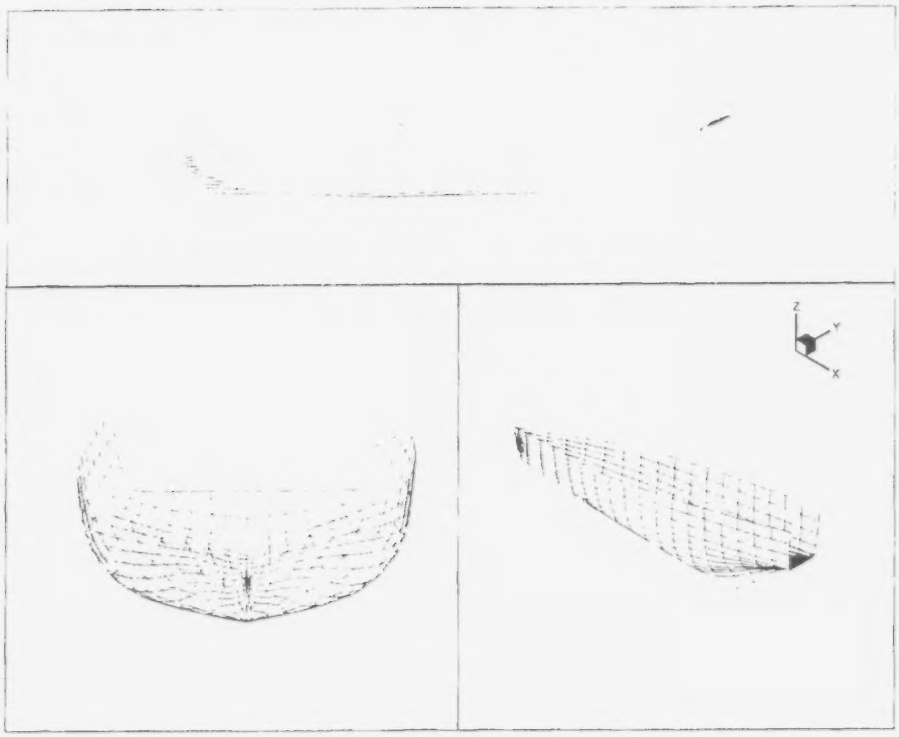

Figure G.3: A CPF Hull heeled by port side 1.5°, trimmed by stern 2.5° and heaved 0.0m (without transom)

P517434.PDF [Page: 89 of 91]

UNCLASSIFIED
SECURITY CLASSIFICATION OF FORM
(highest classification of Title, Abstract, Keywords)

DOCUMENT CONTROL DATA

(Security classification of title, body of abstract and indexing annotation must be entered when the overall document is classified)

1. ORIGINATOR (the name and address of the organization preparing the document Organizations for whom the document was prepared, e.g. Establishment sponsoring a contractor's report, or tasking agency, are entered in section 8)

Martec Limited
1888 Brunswick Street, Suite 400
Halifax, NS B3J 3J8

2 SECURITY CLASSIFICATION (overall security classification of the document including special warning terms if applicable)

UNCLASSIFIED

3 TITLE (the complete document title as indicated on the title page Its classification should be indicated by the appropriate abbreviation (S,C,R or U) in parentheses after the title)

Theoretical manual for SEALOADS version 1.1, a computer program for prediction of nonlinear ship motions, sea loads and pressure distribution in the time domain

4 AUTHORS (Last name, first name, middle initial If military, show rank, e.g. Doe, Maj John E)

Qiu, W., H. Peng, and Hsiung, C.C.

5 DATE OF PUBLICATION (month and year of publication of document)	6a NO OF PAGES (total containing information Include Annexes, Appendices, etc)	6b NO OF REFS (total cited in document)
August 2001	xiv, 68	42

7 DESCRIPTIVE NOTES (the category of the document, e.g. technical report, technical note or memorandum. If appropriate, enter the type of report, e g interim, progress, summary, annual or final Give the inclusive dates when a specific reporting period is covered).

CONTRACT REPORT

8 SPONSORING ACTIVITY (the name of the department project office or laboratory sponsoring the research and development Include address).

Defence Research Establishment Atlantic
PO Box 1012
Dartmouth, NS, Canada B2Y 3Z7

9a PROJECT OR GRANT NO (if appropriate, the applicable research and development project or grant number under which the document was written Please specify whether project or grant)	9b CONTRACT NO (if appropriate, the applicable number under which the document was written)
1gb13	W7707-008063/001/HAL

10a ORIGINATOR'S DOCUMENT NUMBER (the official document number by which the document is identified by the originating activity This number must be unique to this document)	10b OTHER DOCUMENT NOs (Any other numbers which may be assigned this document either by the originator or by the sponsor.)
	DREA CR 2001-176

11 DOCUMENT AVAILABILITY (any limitations on further dissemination of the document, other than those imposed by security classification)

(X) Unlimited distribution
( ) Defence departments and defence contractors; further distribution only as approved
( ) Defence departments and Canadian defence contractors; further distribution only as approved
( ) Government departments and agencies; further distribution only as approved
( ) Defence departments; further distribution only as approved
( ) Other (please specify):

12 DOCUMENT ANNOUNCEMENT (any limitation to the bibliographic announcement of this document This will normally correspond to the Document Availability (11) However, where further distribution (beyond the audience specified in (11) is possible, a wider announcement audience may be selected)

UNCLASSIFIED

P517434.PDF [Page: 90 of 91]

13. ABSTRACT (a brief and factual summary of the document It may also appear elsewhere in the body of the document itself It is highly desirable that the abstract of classified documents be unclassified. Each paragraph of the abstract shall begin with an indication of the security classification of the information in the paragraph (unless the document itself is unclassified) represented as (S), (C), (R), or (U) It is not necessary to include here abstracts in both official languages unless the text is bilingual)

This report outlines the theoretical background in the FORTRAN program SEALOADS version 1.1 for computing nonlinear ship motions, bending moments and shear forces on the hull, and hydrodynamic pressure distributions over the wetted hull surface. The computation is carried out in the time domain by using the three-dimensional panel method. A pseudo-nonlinear module is introduced to account for the instantaneous wetted surface. In SEALOADS, the external forces acting on the ship hull include the linearized radiation and diffraction forces, nonlinear Froude-Krylov force, viscous roll damping force, bow-flare slamming force and forces from rudder, maneuvering and propeller. The linearized radiation and diffraction forces are obtained from the impulse response functions, which are solved by using the time-domain Green function and applying a non-impulsive input to the ship. The nonlinear Froude-Krylov force is computed at the instantaneous wetted surface of the hull. A two-dimensional wedge model is applied to compute the bow-flare slamming force. The nonlinear equations of ship motion are solved by the fourth-order Runge-Kutta technique or by the extrapolation method. Effects of position-dependent hydrodynamic coefficients are considered. An automatic panel generator based on NURBS surfaces is also included in this version.

14. KEYWORDS, DESCRIPTORS or IDENTIFIERS (technically meaningful terms or short phrases that characterize a document and could be helpful in cataloguing the document They should be selected so that no security classification is required Identifiers, such as equipment model designation, trade name, military project code name, geographic location may also be included If possible keywords should be selected from a published thesaurus e g Thesaurus of Engineering and Scientific Terms (TEST) and that thesaurus-identified If it not possible to select indexing terms which are Unclassified, the classification of each should be indicated as with the title)

ship motions
sea loads
hydrodynamic pressures
time domain
3-dimensional panel method
computer program
theoretical manual

DCD03 2/06/87-M/ DREA mod. 17 Dec 1997